Development of a Robust Encoding Scheme for Delivering Artificial Sensory Information through an ICMS Electrical Interface

David Atle Bjånes

A dissertation

submitted in partial fulfillment of the

requirements for the degree of

Doctor of Philosophy

University of Washington

2018

Reading Committee:

Chet Moritz, Chair

Josh Smith, Co-Chair

Rajesh Rao

Program Authorized to Offer Degree:

Electrical Engineering, Neural Computation and Engineering

University of Washington

Abstract

Development of a Robust Encoding Scheme for Delivering Artificial Sensory Information through an ICMS Electrical Interface

David Atle Bjånes

Chair of the Supervisory Committee:
Chet Moritz
Departments of Electrical Engineering, Rehabilitation Medicine and Physiology & Biophysics

Current users of brain-computer interface (BCI) technology must rely on visual feedback of cursor or robotic arm movement. The inherently long delays of visual processing likely contribute to relatively slow and unnatural control of BCIs. Despite increasing numbers of electrode sites and ever growing complexity of control algorithms, BCI technology has yet to achieve rapid, dexterous control comparable to an intact human system. We believe the lack of tactile perception and proprioceptive input imposes a fundamental limit on speed and accuracy of BCI-controlled prostheses or re-animated limbs. By artificially recreating this high-resolution pathway via Intra-Cortical Microwire Stimulation (ICMS), BCI stability and control may be substantially improved. Towards this aim, we are exploring cortical sensitivity of modulating stimulation parameters to further understand the critical stimulation features which best encode sensory intensity.

Given the high dimensional parameter space of electrical stimulation, neural interface designers have many options for presenting graded sensation. Parameters such as amplitude, frequency, pulse-width, stimulation train duration, and electrode site could be modulated to vary the intensity of a percept. Using our novel center-out task for rodents as a behavioral metric of perceived intensity, we compare the perceptual resolution of modulating key parameters, both individually and combinatorically. Rodents perform discrimination tasks to measure psychometric curves and just-noticeable-differences (JNDs). Our results show that parameters which modulate the charge-per-pulse (CPP), have the highest resolution while parameters which modulate the frequency of presentations of those pulses have much lower resolution. Amplitude and pulse-width are critical parameters in understanding the mapping between parameter modulation and sensory perception of intensity.

Our overarching goal is to formulate a general pattern for providing a high resolution feedback signal which can be mapped to any sensory modality. Based on our comprehensive exploration of electrical stimulation parameters, we present the state of the art encoding scheme for modulating the sensory perception of intensity.

TABLE OF CONTENTS

LIST OF FIGURES

LIST OF TABLES

ACKNOWLEDGEMENTS

The author would like to acknowledge Dr. Jack Waters and Dr. Doug Ollerenshaw at the Allen Brain Institute for insights with the high throughput training arenas. I would also like to acknowledge Richy Yun, Ryan Kelley, Jasmeet Khera, Oliver Stanley, and Anna Pendleton for help with animal monitoring and behavioral training. Amanda Fischedick, Michael Sunshine and Tom Richner provided invaluable help with surgical protocols and techniques.

DEDICATION

To my parents, Atle and Laura Bjånes; who have ingrained a love of learning and endured years of endless why questions. I will always be grateful.

Chapter 1. INTRODUCTION

1.1 MOTIVATION

Somatosensation plays an essential role in the way we interact with and experience the world around us. Tactile feedback allows us to perform mundane tasks like buttoning our shirts, drinking a cup of coffee, or striking a match without paying deliberate attention to the individual movements of our fingers or arms. Proprioception enables us to perform highly coordinated, practiced movements such as throwing a baseball or playing the piano. Temperature sensitivity can warn us of dangerous surfaces (such as a hot stove or beverage) or remind us to layer up during cold weather. The warmth and pressure we associate with sensation of touch is a primary way many people experience comfort and connection to their loved ones and friends.

Many people with a spinal cord injury (SCI), stroke or amputation have large motor and sensory impairments over significant regions of their bodies. By developing technologies and tools to restore their motor function, the independence and autonomy gained will significantly improve their quality of life. Simultaneously restoring somatosensation will be an essential part to this goal of natural and effortless interactions with the world around them.

Brain computer interfaces (BCI's) have been developed to decode information from the brain for a variety of applications needed by such a patient population (Fetz, 1969; Jackson & Fetz, 2007; Kennedy & Bakay, 1998; Nicolelis & Lebedev, 2009). Development of BCI technology has led to the ability to decode high level goals (Aflalo et al., 2015), control an intended trajectory (Musallam, Corneil, Greger, Scherberger, & Andersen, 2004; Velliste, Perel, Spalding, Whitford, & Schwartz, 2008; Wessberg et al., 2000). Prosthetic (Collinger et al., 2013; Hochberg et al., 2012) or reanimated (Moritz, Perlmutter, & Fetz, 2008) limbs can be controlled

from such an interface. Peripheral nerve interfaces for controlling the bladder and bowl (Navarro et al., 2005) enable volitional control over the GI system, increasing independence and autotomy of many SCI patients. Deep brain stimulators (Malekmohammadi et al., 2016; Widge, Dougherty, & Moritz, 2014), useful for mitigating the symptoms of Parkinson's, essential tremor or psychiatric patients, can be controlled by such an interface in real time to offset side effects of the stimulation.

Historically, much effort has been devoted to the development of these open-loop brain computer interfaces. Studies have focused on decoding trajectory information to drive either a cursor / virtual arm on a screen or a robotic arm, and rely only visual feedback to update the user (Hochberg et al., 2006; Serruya, Hatsopoulos, Paninski, Fellows, & Donoghue, 2002; Taylor, 2002). Such systems have substantially improved in recent years by increasing recording channel counts (Santhanam, Ryu, Yu, Afshar, & Shenoy, 2006; Viventi et al., 2011), complex decoding algorithms (Schalk, McFarland, Hinterberger, Birbaumer, & Wolpaw, 2004) and modeling of the neural networks recorded (Carmena et al., 2003)

Groups at Pittsburgh (Collinger et al., 2013) and Brown University (Hochberg et al., 2012) achieved an incredible 7-10 degrees of freedom control of robotic arms, MPL (Johannes, Bigelow, Burck, Harshbarger, & Kozlowski, 2011) or DEKA arm (Resnik, Klinger, & Etter, 2014). These technical engineering feats have leveraged large channel counts (>100 recording sites) and targeted brain areas (M1) to achieve the state of the art in brain decoding and integration with a meaningful output (robotic arms). However, the heavy cognitive load required to drive these systems and difficulty with fluid control during grasping or object manipulation tasks (Fagg et al., 2007) reminds us that integration of somatosensory feedback could significantly improve control (Bensmaia & Miller, 2014).

Given the complexity of integration of the somatosensory with the motor system at each level (peripheral, CNS, and cortically), there are many proposed solutions for both sensory substitution and biomimetic activation of existing sensory networks (Bensmaia & Miller, 2014). At one end of the spectrum, sensory substitution could be used to train the brain to substitute one modality for another (i.e. using vision to determine the amount of force applied to an object by seeing the deformation of said object) (Bachy-y-rita, Collins, Saunders, White, & Sscadden, 1969). Tactile feedback could be used in a different part of the body (such as the back or arms) as a proxy for an impaired sensation in a lower extremity (Riso, 1999). These techniques have the advantage of being minimally invasive and relatively easy to implement. There are hard limitations with these approaches, the brain does not fully integrate these sensations and responds slowly to their input (Marasco, Kim, Colgate, Peshkin, & Kuiken, 2011).

Biomimetic activation of existing sensory networks in contrast seems far preferable, since it utilizes existing pathways and processing networks. Stimulation through peripheral nerve cuffs in the arm can recreate impaired sensations in the hands (Tan et al., 2014). Recording sensory activation patterns in the brain (Tabot et al., 2013) or spinal roots (D. J. Weber, Stein, Everaert, & Prochazka, 2007) and stimulating them has been successful at recreating sensations of motion, or pressure on the fingertips. While activating peripheral nerves has been highly successfully in generated naturalistic sensations, recreating acquired cortical activation maps through stimulation is highly sensitive to strict laboratory conditions. And for SCI patients with severed connections to the periphery or tetraplegic patients with nerve degeneration, these peripheral interventions are not an option.

1.2 BACKGROUND

For more than 100 years, we have known that electrical stimulation of the brain can evoke sensory perception (Schafer E. A., 1888). Towards integrating this sensory feedback in a closed-loop BCI, these stimulation studies designed encoding patterns to evoke simple circuit activation, inspired by patterns of neural communication recorded in the cortex (Houweling & Brecht, 2008; Kim et al., 2015; London, Jordan, Jackson, & Miller, 2008; Ohara, Weiss, & Lenz, 2004; R Romo, Hernández, Zainos, & Salinas, 1998; Tehovnik, 1996; Venkatraman & Carmena, 2009).

While stimulation patterns are different whether stimulating in the spinal cord (Sunshine et al., 2013), muscle (functional-muscle stimulation) (Moritz et al., 2008), peripheral nerve (Graczyk et al., 2016), or cortex (Kim et al., 2015), they can be described using some fundamental parameters. Electrical stimulation patterns have characteristic parameters amplitude, frequency, pulse-width, number of pulses, inter-train interval, electrode site, and bi-phasic mirrored phases.

1.2.1 *Cortical Stimulation*

Intra-cortical micro-stimulation (ICMS) (Fitzsimmons, Drake, Hanson, Lebedev, & Nicolelis, 2007; R Romo et al., 1998) can deliver these electrical patterns to targeted networks or specific brain areas, while defuse stimulation can be applied through Electrocorticography (ECoG) (Lee et al., 2018; Penfield & Boldrey, 1937; Wang et al., 2013). Both have shown promise in conveying naturalistic sensations, by activating sensory cortical areas in rodents (Fridman, Blair, Blaisdell, & Judy, 2010), primates (O'Doherty et al., 2011a; Tabot et al., 2013) and humans (Flesher et al., 2016; Klaes et al., 2014). While more research is necessary to

directly compare epi-cortical vs intra-cortical stimulation, penetrating micro-wires are in close proximity to neurons and thus may have better control for specific neural network activation.

Prior studies have shown a variety of sensations can be evoked by graded ICMS stimulation delivered to primary sensory cortex. Information can be coded by amplitude modulation (Berg et al., 2013), frequency modulation (Dadarlat, O'Doherty, & Sabes, 2015; Fridman et al., 2010; R Romo et al., 1998; Thomson, Carra, & Nicolelis, 2013) and temporal spike trains (Mackevicius, Best, Saal, & Bensmaia, 2012; A. I. Weber et al., 2013), pulse width (Kim et al., 2015), and electrode site (Fitzsimmons et al., 2007).

Due to the large number of possible parameters (frequency, amplitude, pulse width, train duration, electrode site and others) and the lack of a cohesive model for the effects of changing each parameter in the literature, these prior experiments only explored discrimination of either disparate stimulation patterns, or simply identified the threshold of perception of stimulation. None of these encoding methods have ever been compared directly in the same task and animal model to determine which scheme maximizes information transfer. Nor has a systematic comparison of the perceptual resolution of modulating each parameter been performed.

1.2.2 *High-Resolution Feedback*

To create the maximal fidelity of artificial cortical sensory encoding, we must first understand the optimal method and amount of information that can be transferred to the brain via electrical stimulation. Given there are nearly infinite numbers of ways to construct an electrical stimulus, we have constructed a standard framework to analyze the brain's comprehension of a baseline stimulation pattern. This framework can describe most stimulus patterns commonly found in the literature, defined as a set of parameters in a high dimensional space. In our novel approach, we will measure the brain's ability to detect changes to the pattern by manipulating

each parameter independently, isolating the contributions of each. By capturing the just-noticeable-difference (JND) measurements of each parameter, we can construct a sensitivity manifold across the high dimensional space. This will be the first comprehensive comparison of parameters all in the same animal and at same electrode site. This data will allow us to fairly compare sensitivity across parameters, and identify which stimulus feature spaces have the highest sensitivity. A high resolution encoding model can be validated by mapping the highest resolution parameters to the desired signal to input to the brain.

1.3 Thesis Overview

The dimensionality problem of such a large parameter space necessitates an experimental paradigm that can be largely automated and scalable for the collection of a reasonably large data set across many subjects. We chose the rat animal model due to its rapid learning capabilities, ability to perform complex tasks, and suitableness for replicating our findings across animals. The task was a novel modified center-out task, developed specifically for ease of training, scalable complexity, and automation. This task enables us to quantify perception of sensory stimulation modulation patterns.

Rather than cue the animal for a particular target, stimulation will provide sensory feedback in response to joystick position, mimicking a robotic or re-animated limb providing real-time sensory feedback to a user. The animal will perform a discrimination task between a high and lower magnitude stimulus by exploring several targets in the workspace. We can correlate performance of our task to comprehension of the encoded signal, yielding a qualitative measurement of the perceivable resolution between two points in our high dimensional space. Development of this behavioral paradigm constitutes Chapter 2 of my thesis.

Goal 1: *Development a high-throughput behavioral task to assess comprehension of artificial sensory stimulation.*

From our constructed stimulation framework, five dimensions can be varied independently to convey information to the brain, including amplitude, frequency, pulse width, train interval, and pulse train length. Rather than subsampling the high dimensional space by comparing pairs of disparate stimulation patterns, we strategically sought to fully explore each parameter individually. Our goal was to determine the perceptual resolution of each parameter in order to inform the optimal encoding of sensory feedback. Chapter 3 constitutes the results of that exploration.

Goal 2: *Rigorously evaluate the resolution of modulating each stimulation parameter individually through stimulation delivered via ICMS in sensorimotor cortex.*

In order to facilitate a quantitative comparison of maximum signal resolution, learning rate, and peak performance achievable, we first identified perceivable ranges of each stimulation parameter modified, as well as determining the optimum ranges for maximum information encoding.

By comparing stimulation paradigms found in the literature and novel paradigms outlined below, we gained insight into cortical processing of neighboring circuits and the comparisons between them. By explicitly comparing the ability of the rat to perform the discrimination tasks, we could empirically measure the achievable resolution of a particular encoding paradigm.

Although there is a large parameter space of possible stimulation patterns, our preliminary data suggested that there may exist a lower subspace or plane used by the brain to interpret stimulation. After concluding these single parameter modulation experiments, we strategically explored the contributions of the highest resolution parameters in combination. By co-modulating them, we could determine what specific temporal or spatial features the brain

cued on within the parameter space. To maximize resolution of the input signal delievered to the brain, we identify the primary artificial stimulation features to which cortical networks respond.

Goal 3: *Identify a lower dimensional subspace which predicts the measured resolution of an artificial sensory stimulus presented with ICMS.*

We tested our hypothesis in Chapter 3.3.5 that a reduced subspace exists, by modulating amplitude and pulse-width parameters simultaneously, teasing apart the contributions of modulating each parameter individually. We found that modulating the charge-per-pulse yielded substantially higher sensitivity measurements than modulating parameters which modified the temporal aspects of the stimulation pattern.

1.4 SUMMARY

Towards our goal of developing a high-resolution sensory feedback signal delivered via electrical stimulation to the sensorimotor cortex, we measured the resolution of many types of graded stimulation encodings in the same animal and at same electrode site. Collecting this data set allowed us to directly compare encoding paradigms, yielding insights into development of the return path of bi-directional brain computer interfaces and a platform for further design of efficient electrical stimulation of sensory cortical areas.

Chapter 2. AUTOMATED CENTER-OUT RODENT BEHAVIORAL TRAINER

2.1 INTRODUCTION

Animal models have long been a proxy for studying complex human behaviors such as decision making (Platt & Glimcher, 1999), perceptual discrimination (Newsome, Britten, & Movshon, 1989; Shadlen & Newsome, 2001), motor-skills (Tanji, 2001), cognitive executive functions (Brady & Floresco, 2015; Endo et al., 2011; Poddar, Kawai, & Ölveczky, 2013), learning (Endo et al., 2011; Poddar et al., 2013), memory (Endo et al., 2011; Poddar et al., 2013), and social behavior (Nadler et al., 2004). During the last century, as neuroscience has evolved to study the networked activity of neurons in the brain and spinal cord, much effort has been devoted to understanding the relationship between measured neural activity and external stimuli. However, studying complex processes such as decision-making, executive functions, and memory requires some measureable external behavior for researchers to quantify an animal's internal state. Thus, trained behavioral tasks have become the preferred domain for studying these systems.

Due to inherent variability of these behaviors, researchers must record many observations of each experimental condition. These conditions must be replicated precisely in order to reduce variability of results. To eliminate artifacts arising from laboratory specific protocols and/or experimenters (Crabbe, 1999), a myriad of automated behavioral chambers have been developed to standardize experiments and precisely record an animal's behavioral responses (Brady & Floresco, 2015; Endo et al., 2011; Fenrich et al., 2015; Mohebi & Oweiss, 2014; T. H. Murphy et al., 2016; Nadler et al., 2004; Oh & Fitch, 2017; Poddar et al., 2013; Schaefer & Claridge-Chang, 2012; Torres-Espín, Forero, Schmidt, Fouad, & Fenrich, 2018; Wong, Ramanathan, Gulati, Won, & Ganguly, 2015; Zemmar, Kast, Lussi, Luft, & Schwab, 2015; Zheng & Ycu, 2012).

Studies of these internal systems have historically used non-human primates due to their similarities in cortical structures (Kalaska, Scott, Cisek, & Sergio, 1997) to human brains and complexity of their possible responses. Due to regulatory and funding hurdles, large scale primate experiments are prohibitively difficult to complete (Goodman & Check, 2002; Lankau, Turner, Mullan, & Galland, 2014). Recent rodent experiments have revealed surprising cognitive ability as they have accomplished tasks previously thought only completable by primates (Ölveczky, 2011). Rodents can learn probabilities of reward ratios in various game theory experiments (Kepecs, Uchida, Zariwala, & Mainen, 2008; Viana, Gordo, Sucena, & Moita, 2010; Zeeb, Robbins, & Winstanley, 2009) and visual object recognition (Zoccolan, Oertelt, DiCarlo, & Cox, 2009), perform multi-sensory integration (Raposo, Sheppard, Schrater, & Churchland, 2012), apply rules learned in different contexts (R. A. Murphy, Mondragon, & Murphy, 2008), succeed in sensory discrimination (Uchida & Mainen, 2003), and manipulate a 2D joystick (Slutzky & Jordan, 2010).

These complex tasks, however, often require precise timing, such as the manipulation of a lever or nose poke, or measurement of position in an arena. For rodents, automated behavioral chambers designed to control the precise timing and measurements of each element of the task can eliminate the tedious and error prone bias of human monitoring (Crabbe, 1999).

Automated rodent chambers often use several classic paradigms to record behavioral outputs, requiring animals to pull levers (Brady & Floresco, 2015), retrieve pellets (Fenrich et al., 2015; Wong et al., 2015; Zemmar et al., 2015), or move in the cage, using an array of sensors including video capture (Oh & Fitch, 2017), infrared beams (Thomson et al., 2013), nose-pokes, licking ports and/or joysticks. One of the most complex motor tasks developed for primates is a center-out reaching task (Georgopoulos, Kalaska, Caminiti, & Massey, 1982). This task has

begun to be adapted for rodents (Slutzky & Jordan, 2010), and we build on this work here by modifying the task, automating the training, and demonstrating success in many animals.

Our Automated Center-out Rodent Behavioral Trainer (ACRoBaT) device (Figure 2.1) provides a fully automated 23-step algorithm to train naïve rats to perform a modified version of the classic center-out task. Custom hardware allows 13 possible target locations arranged in a bottom half circle, and we show training data from 18 rats learning a three-target choice task (Results Section: 3.4). We employ several key strategies to accelerate the learning process, including:

1. Adaptive Target Selection to prevent development of repetitive motor patterns during the target search portion of the task
2. Adaptive Timeout to introduce a dwell requirement for target selection
3. Soft Start and Intermittent Rewards to increase motivation through the session

These algorithms are fully instantiated on each device, while the experimenter can modify parameters and log relevant variables as needed via a desktop computer. Human interaction is limited to selecting the current training step and then placing the animal in a behavioral arena for an hour-long training session. The ACRoBaT device has a flexible code framework for modifications so that the system is easily extendable via open source software. Built from 3D printed components, we believe this device can be easily adopted by labs and can drastically reduce the labor required for high-throughput rodent research, providing a low cost, open source tool for complex neuroscience experiments to our community.

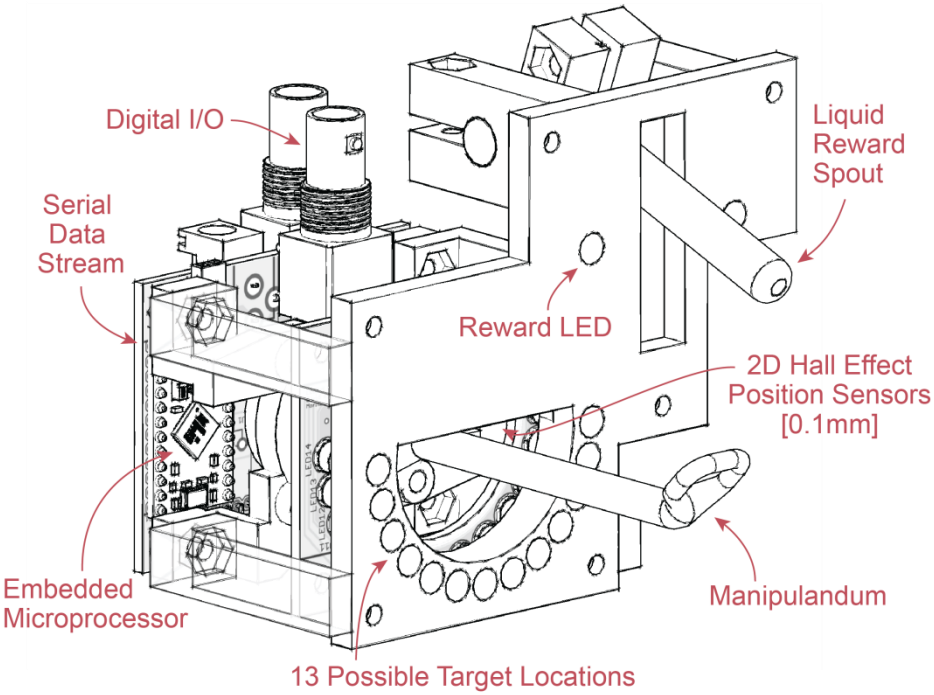

Figure 2.1. CAD drawing of the ACROBAT device.

Two custom PCBs fastened to a 3D printed housing are attached to the front of the cage or arena. A half ring of 13 LEDs are controlled by MAX6966 LED driver chips on the front PCB. The rear PCB handles the capacitive sensor attached to the liquid reward tube, inputs from the 2D hall-effect joystick, connections for the Arduino Pro-Micro running custom C code and digital BNC connections (additional I/O ports). A small 3D printed joystick protrudes into the cage or arena and can easily be manipulated by a rat, with a spring return to the home position. Entire form factor is approximately 10 cm x 7 cm x 5 cm (width x height x depth). Although the device can operate autonomously for training, it must be tethered to a computer via a USB cable to log relevant variables at 100Hz to a text file.

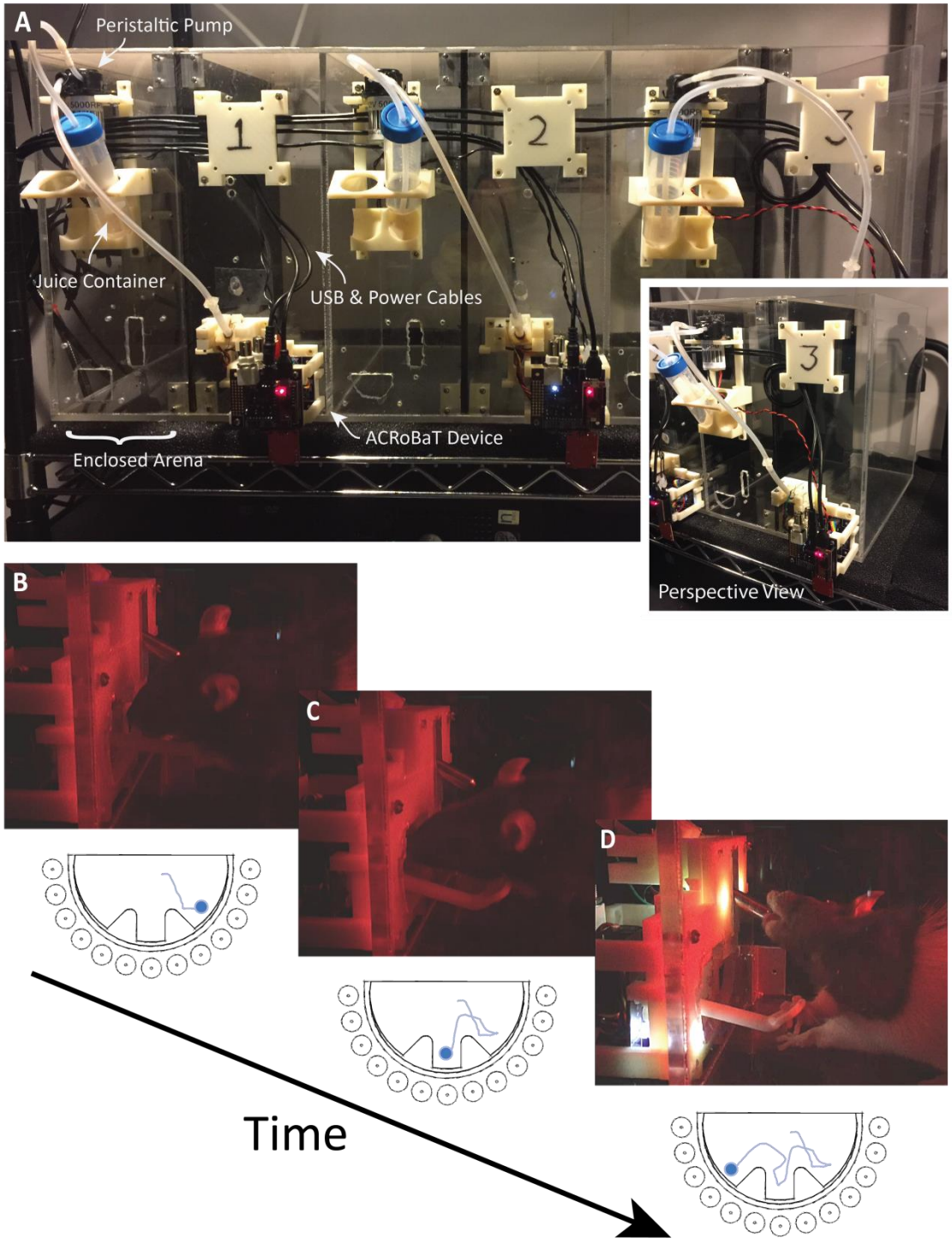

Figure 2.2. Arena Assembly and Behavior

PART A: Three behavioral arenas set up for automated training. Each self-contained arena has an ACRoBaT device near the floor of the enclosed training space, a peristaltic pump to deliver

apple juice rewards, and a power and USB cable to connect the ACRoBaT device to a computer for data logging.

PART B-D: Example images of a rat manipulating the joystick to each of the three targets. Trajectories below show example progress through workspace during a single trial (see Supplemental Videos 1 – 3 for more examples).

2.2 METHODS AND MATERIALS

An automated 23-step training device (Figure 2.1) has been developed for training naïve rats to grip a joystick with their paw and move in a two dimensional space (bottom half of a circle). This protocol requires minimal human oversight, enabling an accelerated training timeline of 2-4 weeks. Visual cues provide sensory feedback about the target location during exploratory motions of the handle. After completing the training, animals will move the handle to and dwell in a specified window about the correct target for 1.25 seconds to obtain a liquid reward (Figure 2.2B).

The Automated behavioral arena is built with 3D printed components to allow for easy modification and scaling to parallel training (Figure 2.2). A military grade Hall Effect 2-axis joystick captures paw position within 0.1 millimeters and a capacitive sensor to indicate animal contact with a liquid reward spout. Both sensors interface with custom PCBs to an Arduino microcontroller. A finite state machine (FSM) processes all variables (Figure 2.3) to track animal progress and dispense rewards via a peristaltic pump. To log behavioral data variables, each device can be tethered to a desktop computer running a custom C++ program. Data is streamed via a serial connection at 100Hz to a CSV text file on the desktop computer.

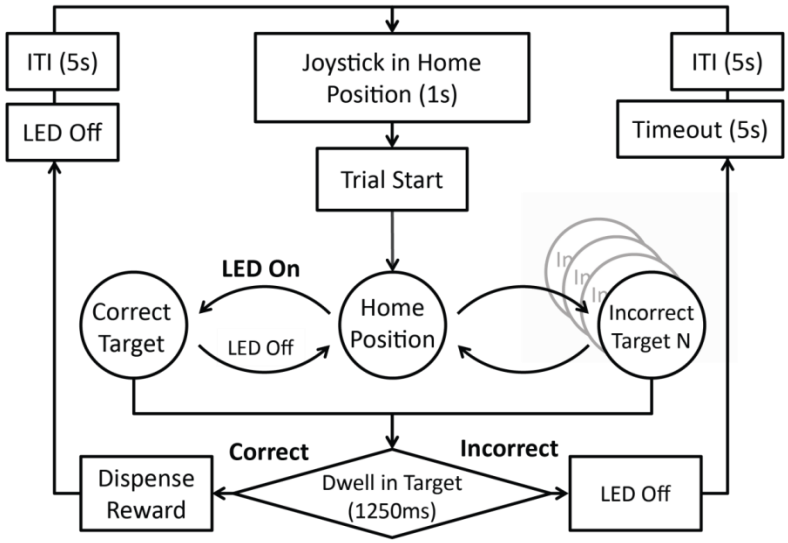

Figure 2.3. Flow chart of finite state machine (FSM) of final stage of task training

Block diagram shows a single trial progression and each stage of the trial. Trial starts once joystick remains in home position for more than 1 sec, and concludes when animal dwells in a target for more than 1.25 sec. If the target is correct, a liquid reward is dispensed, and the Inter-Trial-Interval (ITI) allows a new trial to start after 5 seconds. If the target was incorrect, an additional timeout penalty of 5 seconds is applied. These values are specified for our particular experimental paradigm, but each are customizable for a variety of applications. In our protocol for example, several variables including dwell in target time and LED turn on time, are modulated to progressively to increase task difficulty over time.

2.2.1 *Animals*

We trained adult female Long-Evans rats chosen for their ability to perform complex tasks (Whishaw, Gorny, Foroud, & Kleim, 2003). Animals were group-housed (Charles River, 200-300g) during training (1-3 animals per cage). To habituate animals to the arena and human handling, we gave solid sugary food rewards (Kellogg's Froot Loops or Reese's Choco Puffs). We set the housing room light cycle to a 12 hour day/night cycle, shifted such that the housing and behavior room was dark from 9am-9pm. This permitted training/testing to take place during the animals' active, dark cycle. We allowed ad libitum access to food throughout the training, but completely restricted animals from water in their home cages. We gave free water for ½ hour each day of restriction following completion of their training/testing sessions. For correctly completing a trial during the behavioral task sessions, we administered drops of apple juice as a liquid reward (0.05 ml). On weekends, we gave each animal free access to water. We weighed animals each day of restriction to ensure adequate growth for young animals and maintenance of body weight for older animals. All procedures were approved by the University of Washington IACUC.

2.2.2 *Behavioral Arena and Task Design Caption*

A clear rectangular acrylic box (12'' length x 8'' width x 18'' height) was outfitted with an ACRoBaT device, including joystick, housing and Arduino boards, as well as a pump dispenser and liquid reward tubes mounted to the front of the arena (Figure 2.2A). Range of motion for the joystick was a semicircle with a 4 cm radius, centered on the front wall 5 cm from the floor of the arena. The liquid reward sipper tube was centered in the arena, positioning the joystick predominately on one side of the animal. This encouraged the animal to use a single forepaw to manipulate the joystick. The ACRoBaT connected to the computer via a micro-USB cable. A

12V+ barrel jack cable powered the device, and a two-wire cable connected the pump to the ACRoBaT. Two additional BNC or a DB25 are available for synchronizing each ACRoBaT to external hardware such as motion capture or neural recording devices. LED's on the ACRoBaT indicated trial start/stop times as well as the timeout periods following incorrect trials. The arena was lit with only red lamps in a darkened room to aid the experimenter in observing the animals. A lid was placed over the arena to prevent the animal from jumping out, and contained small holes for fresh air and to prevent condensation build-up.

While a traditional center-out task would have included a full circle of targets, we arranged our targets in a downward semi-circle. This was done because the rats were unable to push the joystick above their heads given the placement of our joystick in front of the animals. A traditional center-out task would also present the cue prior to start of joystick movement rather give a feedback signal while the animal is exploring the targets. All animals learn to move to a cued target as part of the training protocol detailed below. They then progress to search for 'hidden' targets. If the cued version of the task is desired, however, our flexible code framework can easily be modified to train animals to move to and dwell at the pre-cued target.

The ACRoBaT task does not restrict paw usage, and animals can use either forelimb to manipulate the joystick. Here we present data collected in left-handed arenas, with joystick on the left side of the sipper tube. We have included device designs with the joystick on either the left or right side of the sipper tube if desired (Results and Discussion: Section 3.6).

2.2.3 *Software and Data Analysis*

Each ACRoBaT device is run by its own Arduino microcontroller. Programmed with custom C code, they can independently handle all training steps. Additionally, to log behavioral data and training variables, each device can be connected to a C++ logging program on a personal

computer via a serial interface. Many arenas can be independently controlled by a single desktop computer, limited only by the number of USB ports and computer RAM. Seven ACROBAT devices were simultaneously connected to a 3GHz processor with 4GB of RAM, and no dropped data points, lag issues or serial disconnections were observed.

Behavioral variables were sampled at 100Hz and logged in a text file. The log file consists of a comma separated value (CSV) file containing program variables. All post processing was performed in Matlab (The Mathworks). For all statistical tests, a two-sample t-test was used with $p < 0.01$ considered significant.

2.2.4 *Training Protocol*

Each training session lasted approximately one hour or 200 trials, whichever came first. Sessions generally started at the beginning of the dark cycle and/or at the end of the dark cycle (either once or twice a day) to maximize motivation. Animals were placed into the behavioral arena, while the researcher selected the appropriate training step using the software on the personal computer. The 23 steps are divided into four distinct phases, and we specify each training step in detail below (Supplemental Video 3 illustrates example trials in each of the 4 phases). Each step is fully implemented and automated, so the human researcher needs only to select the training step for each session and then can return after the hour of training is complete.

2.2.4.1 Pre-Training

- **Step 1:** If animals were obtained from an outside vendor, we acclimatized them after transport for a minimum of one week (Endo et al., 2011), giving ad libitum food and water. Handling animals during this time helps speed up the acclimation process.
- **Step 2:** After the one week acclimatization period, we began liquid restriction, increasing by 4 hour increments per day (day 1: restriction for 4 hours, day 2: restriction for 8 hours, etc.)

until water is restricted at all times except when the animal is performing the task, and for 30 min following training completion each day.

2.2.4.2 Training

We trained each animal according to the protocol detailed below. Sessions lasted approximately one hour, during which time the automated device handled all interactions with the animals. We only needed to place the animal in the cage and select the initial training step. Table 1 details the criterion for successfully completing each training step and advancing to the next automated step.

Table 2.1. ACRoBaT Protocol

Step #	Criterion for Completing: Trial	Training Step
Phase 1: Acclimation and Move Joystick		
1	Lick sipper tube for 20 milliseconds to complete the trial.	After a single session with at least 100 trials, step is complete.
2	Lick sipper tube 10 times to complete the trial.	After a single session with at least 100 trials, step is complete.
3	Move joystick handle 2 cm from center in any direction to complete the trial. Dominant target preferred by the animal (Left or Right) identified.	After one session of at least 100 trials, advance to next step.
Phase 2: Cued to Move Joystick to One of Two Targets		
4	Move joystick to only the non-dominant target to complete the trial. Correct target indicated by illuminated LED during entire trial, while incorrect target is not illuminated. No penalty for moving joystick to incorrect target. (Physical dividers for guiding movement to the correct target are optional during Phase 2 steps.)	After one session of at least 100 trials, advance to next step.
5	Move joystick to only the previously identified dominant target to complete the trial. Correct target indicated by illuminated LED during entire trial, while incorrect target is not illuminated. No penalty for moving joystick to incorrect target.	After one session of at least 100 trials, step is complete.
6	Move joystick to the correct target (Left or Right) to complete the trial. The correct target is randomly selected per trial and indicated by illuminated LED during entire trial. The incorrect target is not illuminated. There is no penalty for moving joystick to incorrect target.	After two consecutive sessions with at least 100 trials each, step is complete.

Phase 3: Cued to Move Joystick to One of Three Targets		
7 (optional)	Introduce another target (Center, Top Left, or Top Right, etc.). Move joystick to the new target to complete the trial. Correct target indicated by illuminated LED during entire trial, while incorrect targets are not illuminated. No penalty for moving joystick to incorrect targets.	After one session of at least 100 trials, step is complete.
8 (optional)	Move joystick to randomly selected correct target (either Left, Right, Center, etc.). Correct target is indicated by illuminated LED during entire trial, while incorrect targets are not illuminated. No penalty for moving joystick to incorrect targets.	After two consecutive sessions with at least 100 trials each, step is complete.
Repeat Steps 7 & 8 for each additional target. Method tested for up to three targets.		
Phase 4: Find Target and Select by Dwelling with Joystick		
9	Move joystick to find randomly selected correct target (Left, Right, Center, etc.). The correct target illuminates via LED only when joystick is in target, while incorrect targets' LEDs are never illuminated. Animal must dwell in correct target for 250 milliseconds to receive a reward, and a timeout period initiates if animal dwells in an incorrect target for more than 30 seconds.	After a session completed with at least 100 trials and accuracy of above 75% (two targets) or 66% (three targets), step is complete.
10	Same as Step 9, except the timeout period initiates after dwelling for 5 seconds in an incorrect target. Soft Start and Adaptive Timeout strategies begin at this step (Results & Discussion Section: 3.2 and 3.3).	After a session completed with at least 100 trials and accuracy of above 75% (two targets) or 66% (three targets), step is complete.
11 - 15	Same as Step 10. For each successive step, the correct target dwell time starts at 400ms, 550ms, 700ms, 850ms, and 1000ms respectively. At the same time, for each successive step, the incorrect target dwell time begins at 4 sec, 3 sec, 2 sec, 1.75 sec and 1.5 seconds. These values change during the session as animal accumulates correct trials according to the Adaptive Timeout strategy (Results & Discussion	After a session completed with at least 100 trials and accuracy of above 75% (two targets) or 66% (three targets), step is complete.

	Section: 3.2). During **Steps 12-15**, the Intermittent Reward strategy is employed (Results & Discussion Results 3.3 section).	
16	During the final task, the animal must dwell for 1250 milliseconds in correct target to receive a reward and timeout period initiates if the animal dwells for 1250 milliseconds in any incorrect target.	After a session completed with at least 100 trials and accuracy of above 75% (two targets) or 66% (three targets), step is complete.
Phase 5: Replace LED Cue with Stimulation, Odor, Audio or Other		
17-23 (optional)	Same protocol as Steps 9-16, except using a different cue other than the LED's such as odor, audio tones, electrical or optical stimulation, tactile cueing, etc.	See Steps 9-16

2.2.5 *Replace LED Cue (Stimulation, Odor, Audio or Other)*

At this point, the fully trained animal can perform an n-target modified center out task. They are actively searching for the correct target, and using the illuminated LED to identify the correct target before deciding on which target to ultimately select. If the end user would like to train a classic center out task (cue presented prior to start of trial, rather than as feedback), a simple setting in the code can be changed (see documentation in Results and Discussion Section 3.6).

As an optional extension to this protocol, steps 17-23 enable the end user to use audio, odor, pharmacological, optical, tactile or intra-cortical micro-stimulation (ICMS) instead of LED cues as desired by the experimental system under study (data not included).

2.3 Results and Discussion

We have successfully trained 18 rats with various modifications to the training procedure to assess the improvements in performance. Three rats trained without our motivational and adaptive timeout strategies, three rats trained using motivational and adaptive timeout strategies, and 12 rats trained with both strategies and a high-resolution 2D hall-effect joystick.

2.3.1 *Strategy I: Adaptive Target Selection*

We discovered that training time substantially decreased by using an Adaptive Target Selection strategy. Rats have a difficult time with delayed gratification and easily develop "habits" or "patterns" which they robustly follow to achieve a reward. In order to encourage them to break these habits and continue searching for a new target (i.e. stop repeatedly going to a single target), subsequent correct targets were selected based upon recent performance. For example, if the animal had a choice between targets A and B, and they had correctly selected target A only 30% of the time during the last 20 trials, there would be a 70% chance target A would be selected as the next target.

2.3.2 *Strategy I: Adaptive Target Selection*

We also discovered that requiring progressively longer dwell times resulted in much quicker learning of the dwell portion of the task. The Adaptive Timeout strategy successfully trained rodents to dwell in a particular target for a reward, rather than just receiving an instantaneous reward for reaching the correct target (Figure 2.4). Each time the rodent completed five trials successfully, the time requirement to dwell for reward increased by 25 milliseconds and the dwell time requirement to trial timeout (dwelling in an incorrect target) decreased by 50 milliseconds. This gradual progression substantially reduced the number of trials and sessions

needed for completion of training compared to the large stepped increases of 150 milliseconds in our original protocol (Methods Section 2.4.3, Step 11).

2.3.3 *Strategies III & IV: Soft Start and Interspersed Easy Trials*

We employed two motivational strategies to encourage the rat to continue engaging with the task for the duration of the session. The Soft Start strategy sets the initial correct dwell requirement to 250 milliseconds and incorrect dwell requirement to 5 seconds for the first 20 trials. When used in the final steps of the training procedure, these easy trials provided initial motivation for animals to engage with the task. These were especially helpful when the task difficulty increased. The Interspersed Easy Trials strategy sets 10-20% of the subsequent trials to easy trials. These easy trials had a correct dwell requirement of half of the current value. These easy trials helped maintain motivation (Miltenberger, Perkins, Weiss, Carrington, & Williams, 2008) over the course of several hundred trials of each session even during very challenging task conditions (Figure 2.4).

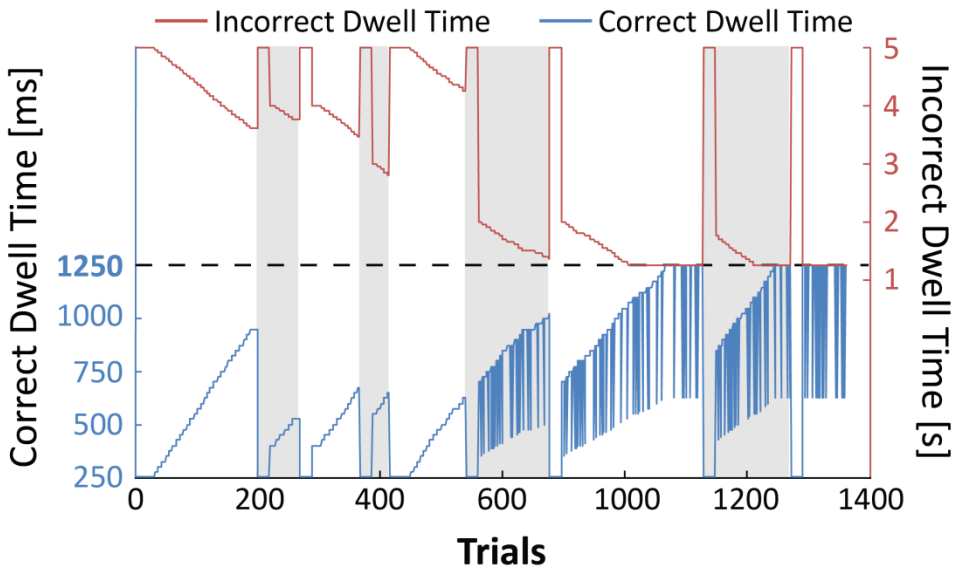

Figure 2.4. Flow chart of finite state machine (FSM) of final stage of task training

Initially, the dwell requirement to select the correct target is much lower than the dwell requirement to select an incorrect target. The incorrect dwell requirement starts at 5000 milliseconds and decreases at a rate of 50 ms per 5 correct trials. The dwell requirement to select a correct target begins at 250 milliseconds and increases at a rate of 25 ms per 5 correct trials. Each day begins with 20 easy sessions with dwell requirements at 250 ms and 5000 ms to encourage the animal to engage in the task. As the animal progresses in the training, the subsequent initial dwell requirements for the correct and incorrect targets are set higher and lower, respectively. During later training levels, we provide 10-20% easy trials to improve motivation. During these easy trials, the dwell requirement for selecting a correct target was halved (sawtooth blue curve from trails 580-1400). Note the different scales on the two y-axes.

2.4 TRAINING TIMES

Each additional strategy resulted in a significant reduction in total training time and improved overall performance. All rats trained to select one of three targets, and all but one animal completed the protocol. Eighteen rats, divided into three groups, demonstrated effects of motivational and learning strategies (Figure 2.5). Group 3, employing strategies I-IV in addition to using a high resolution joystick, performed significantly better than Groups 1 (employing strategies I & IV) and Group 2 (employing strategies I-IV). All groups required significantly less training time than the current state of the art complex rodent behavioral task (Poddar et al., 2013). The number of trials per session ranged from 100-200 and sessions generally finished within one hour (Figure 2.6).

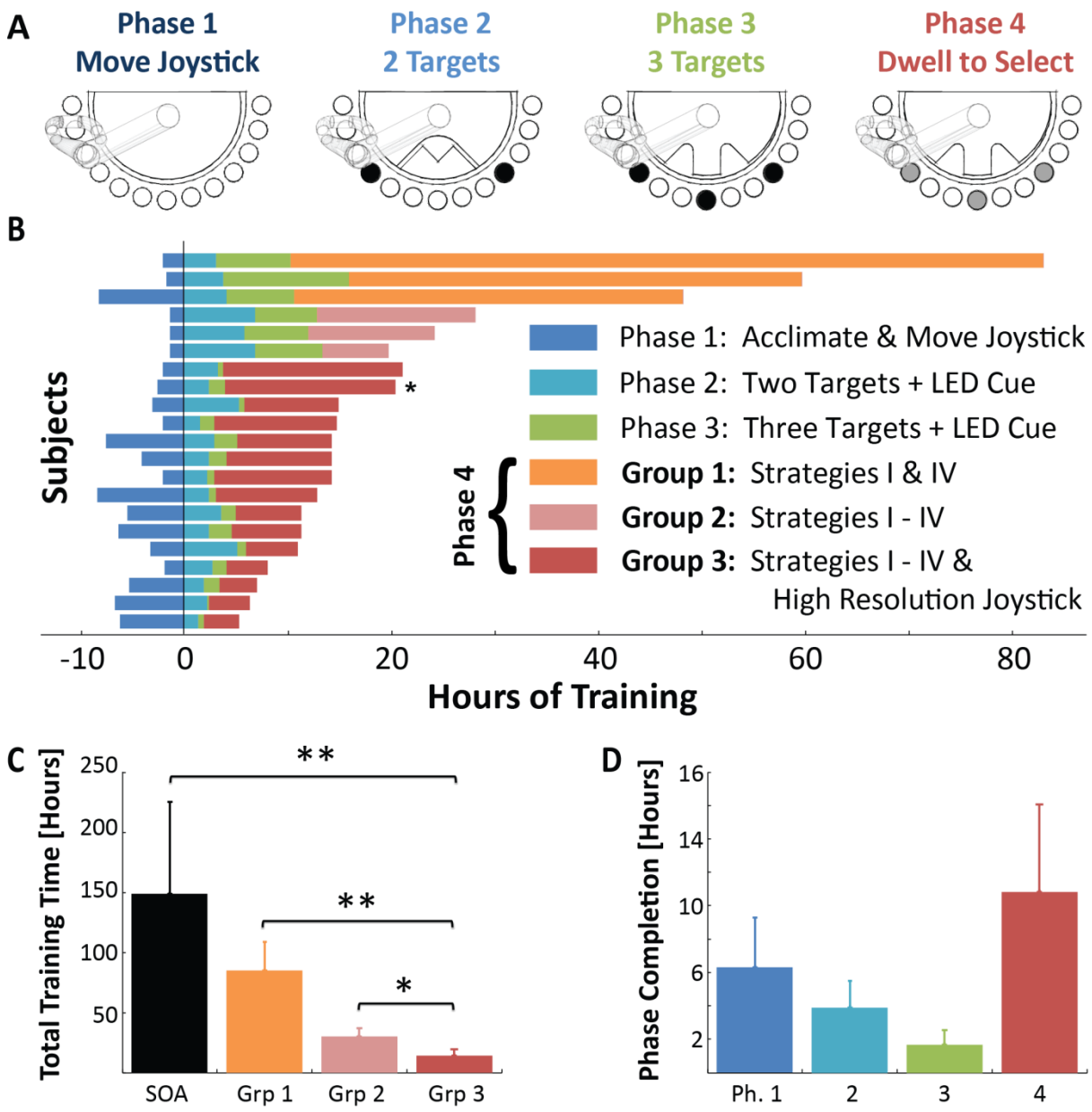

Figure 2.5. Results of ACRoBaT device training performance

PART A: Each animal progresses through four different phases, comprising 3-6 levels. Phase 1 requires the rat to move the joystick towards any of the open circle targets. Phase 2 cues the rat via illuminated LEDs to move the joystick to either left or right targets (randomized per trial). Phase 3 adds a third possible target (center). During Phase 4, LED cues are removed and

the rat is required to search for the correct target. The target LED illuminates only when joystick is in the correct target (randomized per trial). The rat must dwell in a target for 1.25 seconds to make a selection. A liquid reward is given for correct target selections. If the target selected is incorrect, the rat must wait an additional five seconds before starting the next trial.

PART B: Total training times in hours for 18 subjects. Each of the three groups completed the first three phases before completing their individual final training paradigm. Groups 2 & 3 both used training strategies I-IV. Here the amount of time allowed in the incorrect target (before trial ends in an error) is initially much greater than the selection dwell time, and then gradually decreased as correct trials accumulate in a given session. Group 3 used a high resolution joystick (2 degree of freedom hall-effect sensor) rather than a traditional 2D resistor joystick. A single animal (*) was excluded during final phase due to poor learning rates.

PART C: Average training times from naïve to fully trained for the three groups. Group 3 learns the task significantly faster than each of the other groups, and an order of magnitude quicker than the state of the art (SOA) rodent decision making paradigm (a Y-bar left/right decision making task (Poddar et al., 2013)). Error bars reflect one standard deviation. A two-sample t-test was performed between Group 3 and each other group. * $p < 0.01$, ** = $p < 0.001$

PART D: Average time spent on each training phase for group 3. Time to learning the cued joystick behavior requires only a few hours, while learning to search for targets and dwell to select requires about 11 hours. Error bars reflect one standard deviation from the mean.

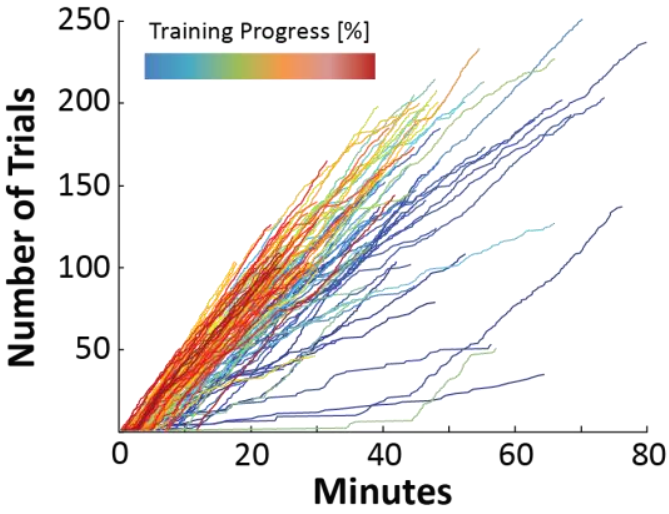

Figure 2.6. Trial successes from a single example animal

Usual sessions last one hour, and animals quickly progress to achieving 5 trials per minute. Typical sessions accumulate 150-200 trials. Animals will sometimes satiate prior to the completion of an hour and then sessions end early. For visualization, sessions occurring early in training are colored blue while later sessions are colored red. Note that as the training progresses, this animal achieves more trials in a shorter period of time. This is remarkable as the trial difficulty is also much higher later in the training protocol.

2.5 Home-Cage Training vs. Dedicated Behavioral Arena

Many recent automated training protocols (Fenrich et al., 2015; Miltenberger et al., 2008; Oh & Fitch, 2017; Poddar et al., 2013) are moving towards in home cage training. The reduced effort of moving the animals from their home cage to their behavioral arena each day and the ability to train all day are attractive. We have no doubt that our ACROBaT protocol could be easily adapted for home cage training. For our current experiments using tethered stimulation, however, we found it advantageous to have a separate arena for training. If the animals need a tether to connect to implanted devices, daily handing provides an easy transition from training to performing the task with a tether.

Context is another important factor. Animals become aware that liquid rewards are only available when placed in the behavioral arena. Lack of water in their home cage motivates them to perform the task when placed in the behavioral arena. If continually exposed to a task in their home cage, animals might train infrequently or may become distracted between trials, rather than training until satiation. The current state of the art rodent decision-making task (Poddar et al., 2013) also showed only minor improvement in efficiency with home cage training, suggesting limits to home cage training.

2.6 Dissemination

So that the community could take advantage of our device, we have assembled a complete list of parts required (Supplementary Material: Table 1) and assembly instructions (Supplementary Material: Instruction Manual). Please visit http://depts.washington.edu/moritlab for appropriate links to download user manual, source code, 3D model files, and PCB board designs.

2.7 CONCLUSION

Complex behavioral tasks for studying processes such as memory, decision-making, and perception have long required primates due to their ability to produce complex responses. Financial, regulatory and labor costs have limited researchers to experiments with small sample sizes and long experimental timelines. Our novel rodent training device, ACROBaT, eliminates many of these hurdles by improving on the state of the art complex behavioral task and dramatically lowering the time and labor costs needed to batch train large numbers of animals. We demonstrate several strategies for significantly improving training times, and delivered a robust protocol free from human bias in monitoring or evaluating performance. By automating each aspect of the trained task, we have enabled rodents to perform a task approaching the complexity to primates, with two to four-week training times in an open-source and flexible environment. This open source, low cost, automated training device lowers many entry barriers for complex behavioral research and can be used for a wide range of applications.

Chapter 3. CHARACTERIZATION OF SINGLE PARAMETER ICMS

3.1 INTRODUCTION

Cortical neuroprostheses offer a unique tool to improve healthcare via bi-directional communication with the nervous system. Although recording neural interfaces have advanced at an exciting pace, the next generation of interfaces will also stimulate the brain in order to convey useful information.

Current brain computer interfaces (BCI)'s can decode neuronal spiking information, enabling subjects to complete a variety of tasks (Aflalo et al., 2015; Fetz, 1969; Hochberg et al., 2006; Jackson & Fetz, 2007; Kennedy & Bakay, 1998; Musallam et al., 2004; Nicolelis & Lebedev, 2009; Serruya et al., 2002; Taylor, 2002; Velliste et al., 2008; Wessberg et al., 2000). Substantial improvements made in BCI technology have incorporated higher channel counts (Santhanam et al., 2006; Viventi et al., 2011), complex machine learning decoders (Schalk et al., 2004) and biomimetic robotic arms (Johannes et al., 2011; Resnik et al., 2014). As a result, human users are able to achieve control of 7-10 degrees of freedom (DOF) (Collinger et al., 2013; Hochberg et al., 2012). However, these open-loop controllers rely on slow visual feedback pathway and could see even greater improvements by incorporating closed-loop sensory feedback (Klaes et al., 2014; Tan et al., 2014).

Achieving naturalistic, coordinated, dexterous control using a BCI will likely require a short-latency, high-fidelity, feedback signal (Bensmaia & Miller, 2014). Prior to incorporating this high resolution sensory feedback in bi-directional neuroprostheses, we seek to understand the parameters of brain stimulation that encode discriminable information.

Direct electrical stimulation of the nervous system has shown promise in conveying sensory information to the brain (Houweling & Brecht, 2008; Kim et al., 2015; London et al.,

2008; Ohara et al., 2004; R Romo et al., 1998; Schafer E. A., 1888; Tehovnik, 1996; Venkatraman & Carmena, 2009). While stimulation patterns are different whether stimulating in peripheral nerve (Graczyk et al., 2016), or epicortical (Johnson et al., 2013) or intracortical cortex (Kim et al., 2015), some commonalities hold. These stimulation studies designed encoding patterns to evoke simple circuit activation, inspired by recorded patterns of neural communication (Tabot et al., 2013). These encoding patterns can be described with five characteristic parameters: amplitude, pulse-width, frequency, number of pulses, train interval.

A variety of sensations can be evoked by graded intra-cortical microstimulation (ICMS) delivered to primary sensory cortex in rodents (Thomson et al., 2013), primates (Berg et al., 2013) and humans (Aflalo et al., 2015; Flesher et al., 2016). Analog information can be coded by modulation of amplitude (Berg et al., 2013; Flesher et al., 2016), pulse-width (Kim et al., 2015), frequency (Fridman et al., 2010; R Romo et al., 1998; Thomson et al., 2013) and temporal spike trains (Mackevicius et al., 2012; A. I. Weber et al., 2013), and varying electrode sites (Fitzsimmons et al., 2007). All have shown some success at discrimination of disparate stimulation patterns; however a comprehensive comparison to determine the highest resolution patterns has not been performed.

To study the fidelity of artificial cortical sensory encoding, we compared the brain's ability to utilize artificial sensory stimulation while individually and systematically modulating each parameter. Prior experiments focused on discrimination of two disparate stimulation patterns rather than exploring the entire parameter space. Early work in ICMS concluded discrimination was possible at very low frequencies (<44Hz) but resolution was poor (Ranulfo Romo, Hernández, Zainos, Brody, & Lemus, 2000). Another study found discrimination between two discrete frequency patterns possible, but it required changing several other parameters to

control for consistent pulse delivery over the specified time period (O'Doherty et al., 2011b). A comprehensive examination of amplitude discrimination was completed in the primate model, but it did not measure discriminability of other parameters (Kim et al., 2015).

Our primary goal was to identify the cortical stimulation patterns which animals could easily discriminate during a forelimb exploration task. We chose to deliver stimulation within the sensorimotor cortex of rats in order to provide an intuitive activation of sensory areas. By measuring just-noticeable-differences of all five different parameters encoding sensory feedback, we aimed to determine which parameter(s) maximizes information transfer. We also compared the perceptual resolution of each parameter in the same task and same animal so that comparisons between parameters can be made.

To convey the maximum sensory information per time, we tested stimulation trains that were brief. Our goal was to determine whether short bouts of stimulation could be perceived by the brain on the timescale of the sensory feedback loop during a motor task (<50ms) (Efron, 1970). We also wanted to test stimulation trains which could both be perceived by the brain and updated much faster than visual feedback (>200ms) (Eric Kandel, James Schwartz, 2014).

We tested the ability to discriminate different cortical stimulation patterns using a modified rodent center-out task (Bjånes & Moritz, 2018). Rather than cue the animal for a particular target, stimulation provided feedback of the joystick position within one of three targets. We used performance of the task as a measure of comprehension of the feedback signal.

Although there is a large parameter space, our choice of animal model and automated task produced a high trial counts per session (200-300 trials), and allowed us to measure and compare single parameter modulation within the same animals and task paradigm. Once the

initial high dimensional manifold of resolution was measured, clear differences emerged between stimulation parameters modulating spatial and temporal features.

Our data suggest there is a lower subspace or plane used by the brain to interpret stimulation. The individual discrimination curves obtained from modulating amplitude and pulse-width showed the highest resolution. Further experiments revealed both parameters may be modulating the same latent variable, charge-per-pulse. Surprisingly, measurements from temporal parameters such as frequency resulted in very low resolution.

3.2 METHODS

3.2.1 *Animals*

Nine adult female Long-Evans rats (Charles River, 200-300g) were trained to perform a modified center-out task (Bjånes & Moritz, 2018). Animals were housed 1-3 per cage during initial training. To habituate animals to the arena and human handling, we gave solid sugary food rewards (Kellogg's Froot Loops or Reese's Choco Puffs). The housing room light cycle was set to a 12 hour day/night cycle, shifted such that the housing and behavior room was dark from 9am-9pm. This permitted training/testing to take place during the animals' active, dark cycle. Ad libitum access to food was allowed throughout the training, but animals were restricted from water in their home cages. Free water was given for ½ hour each day following completion of their training/testing sessions. For correctly completing a trial during the behavioral task sessions, drops of apple juice were administered as a liquid reward (0.05 ml). On weekends, each animal was given free access to water. Animals were weighed each day of restriction to ensure maintenance of body weight. All procedures were approved by the University of Washington IACUC.

3.2.2 *Modified-Center-Out Task*

Each rat followed a 16 step protocol developed to train rats to perform a modified center-out task (Bjånes & Moritz, 2018). Using a 3D printed joystick, rats randomly explored three targets within the workspace. A light cue illuminated when the rat entered the desired target, while no light cue was presented when the rat was exploring non-desired targets. Subjects received a small liquid reward for completion, once they dwelled 1.25 seconds in whichever

target was illuminated. If a rat dwelled for 1.25 seconds in a non-desired target, a timeout penalty of 5 seconds was assessed.

Once proficient at the task, animals could achieve above a 75% success rate in a single session, lasting over 200 trials. Animals were then implanted and the light cue was replaced with direct cortical electrical stimulation.

3.2.3 *Implantation*

Each rat was implanted with an eight by two micro-wire array in sensorimotor cortex. The array was positioned rostral to caudal, 1mm right of bregma (Figure 3.1), 1.5mm deep, targeting layer 5.

An eight by two micro-wire array is soldered to a custom printed-circuit-board (PCB) with mating connector to a DF30 array to vias placed on the bottom of the array. Wires are 30um in diameter with 5 µm thick insulation. Arranged such that the wires in each row are separated by approximately 400 µm, the rows spread by 1.2 mm, the width of the PCB.

The implant was lowered using a stereotax within that window to an approximate 1.5mm depth. Ground wires were wrapped around several skull screws The array (Figure 3.1C) was secured in place using 2-part dental acrylic (C.B. Metabond), exposing the DF-30 connector on top of the array for attachment to cables to record and/or stimulate each electrode.

3.2.4 *Selection of the Electrode Site*

In each animal, stimulation site was chosen corresponding to sensory activity related to the left forepaw, the limb used to control the joystick. Confirming our stimulation site did not trigger muscle or motor units, the activation map of both sensory and motor areas was measured prior to selecting the electrode for each experiment.

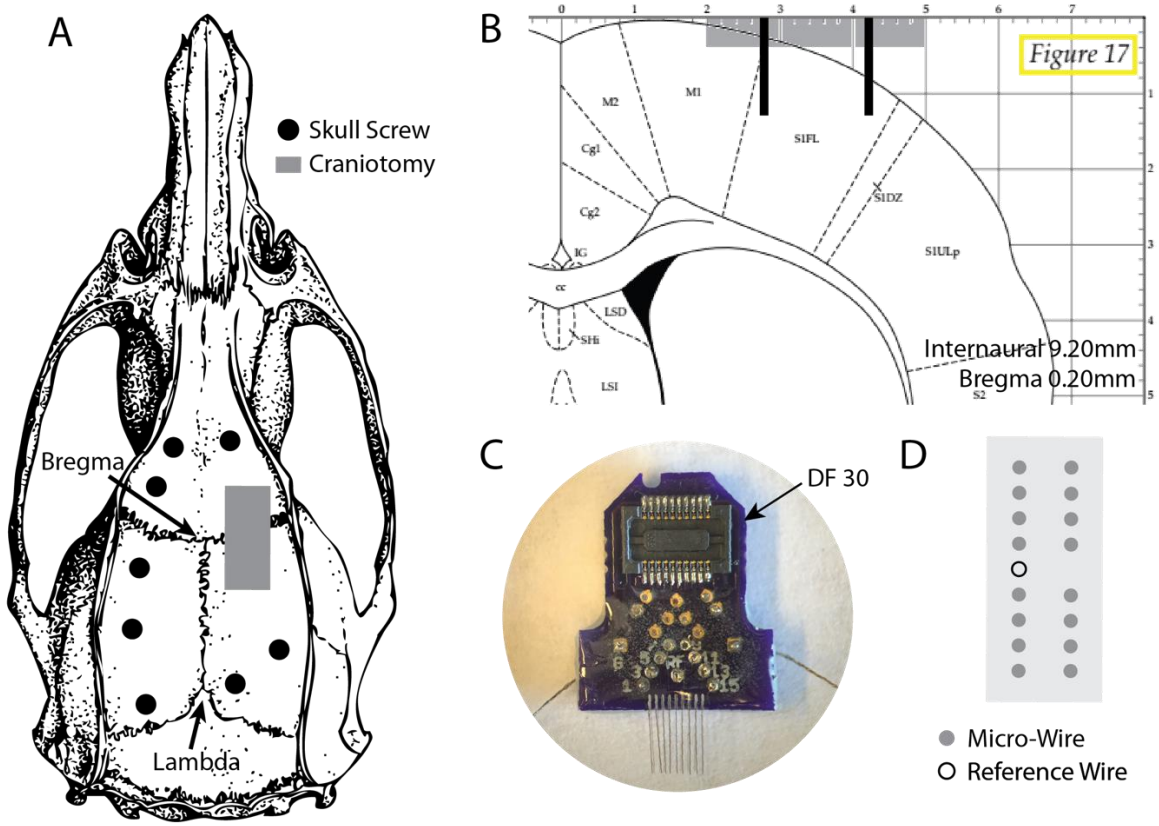

Figure 3.1. Implant Procedure animal

A custom made, 16 channel microwire array was implanted in the left forelimb sensory area, 1.5 millimeters deep. The array was arranged in an 8x2 grid, with a reference electrode in the middle. Two ground wires branched off the array and were wrapped around skull screws (not shown?).

Part A: The placement of seven skull screws is overlaid on cranial landmarks. A 4mm by 3mm craniotomy exposes sensorimotor cortex.

Part B: Coronal slice (Bregma 0.2mm from, Internaural Point 9.2mm) of the targeted cortical implant location. Image adapted from The Rat Atlas (Watson, Paxinos, & Charles, 2005).

Part C: Full view of cortical stimulating array.

Part D: Layout of implanted wires.

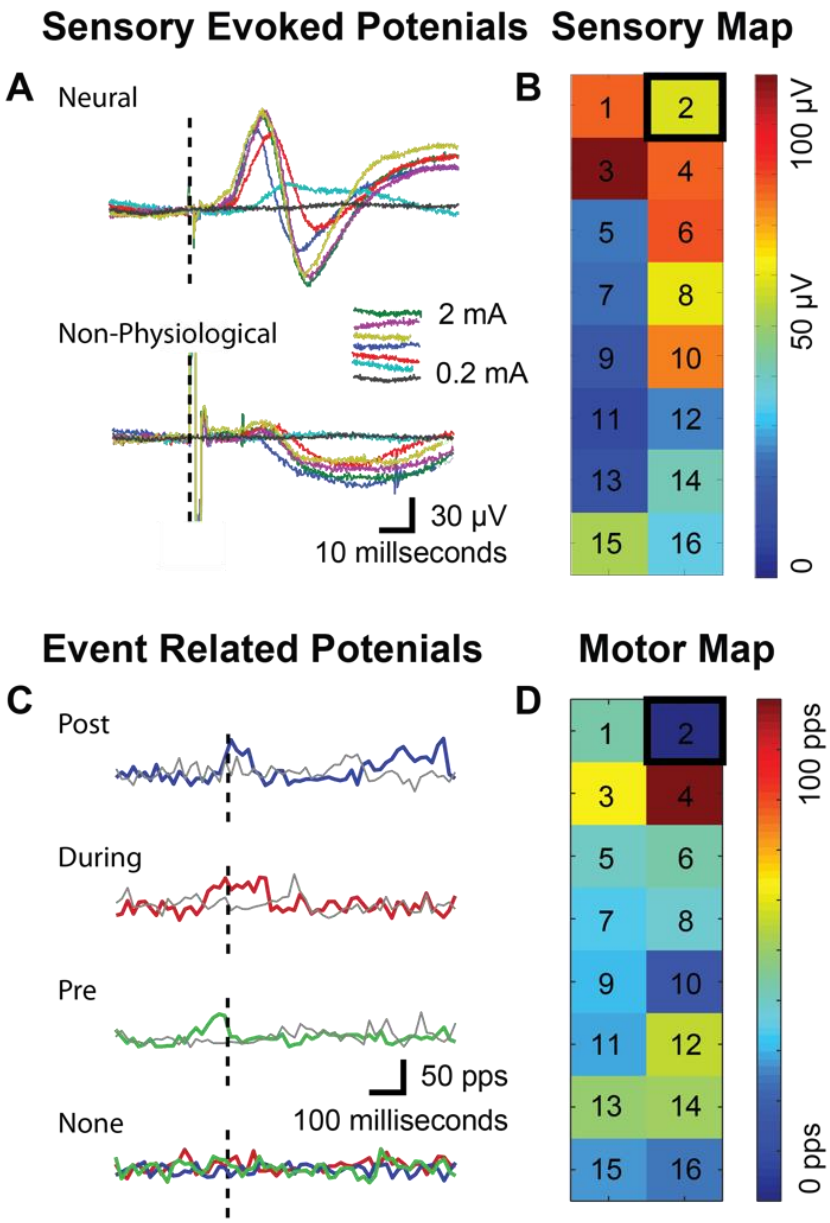

Figure 3.2. Sensory-Evoked-Potentials (SEPs) & Event-Related-Potentials (ERPs)

Part A: Stimulation amplitudes (0.25mA – 2.0mA) refer to biphasic electrical pulses delivered to the bicep muscle on the left forearm. Consistent with sensory conduction velocities, neural signals exhibit a graded response to stimulation about 20 milliseconds after the pulse. Recorded SEPs in sensory areas exhibit biphasic responses and scale to a plateau with stimulation

amplitude (top). Nearby brain areas, non-physiological responses do not evoke a physiological response and exhibit no consistent trends across stimulus amplitude (bottom).

Part B: A heat map shows peak sensory evoked responses on each of the 16 electrodes in response to the same stimulus pulse. From this map, we identify candidate electrodes for our experiment, such as channel 2 for this animal.

Part C: Recorded ERPs for various behavioral events during the task (such as entering/exiting a particular target). Light cues were used for task feedback during the recordings. ERPs were measured by thresholding and smoothing the firing rate from detected single units. A snap-shot of the firing rate was averaged over behavioral features.

Part D: Heat map corresponding to the strength of response above baseline, to visualize electrode sites dominated by motor correlated activity. If we detected activity such as clear excitation post-event (A), sustain during event (B) or pre-event (C), these sites were excluded from possible selection for the experiment. The majority of sites showed no correlation.

3.2.5 *Sensory Evoked Potentials*

In each animal, we measured sensory evoked potentials (SEPs) and event related potentials (ERPs) to verify final electrode location with the implanted cortical region. Animals were lightly sedated using ketamine and xylazine. The left forearm was shaved and two skin electrodes attached one either side of the bicep muscles. We recorded Local Field Potentials (LFPs) at a variety of bicep stimulation amplitudes to test for proportional neural responses, such as increases in onset and amplitude to larger inputs. Some sites showed no correlated activity, with little variation in response to the changing stimulation amplitudes (non-psychologic responses in Figure 3.2A). Biphasic electrical pulses were delivered to the left bicep muscle with amplitudes from 0.25mA – 2.0mA. Based on conduction velocities, we see the cortical SEPs showing a graded response to stimulation about 20 milliseconds after the pulse. A heat map shows peak neural responses (Figure 3.2B) on each of the 16 electrodes in response to the same stimulus pulse. From this map, identification of candidate electrodes for our experiment was possible. For the example animal shown, the electrode site was channel 2.

3.2.6 *Event Related Potentials*

To identify any potential motor activity, animals performed the center-out task using light cues while we captured neural activity. Event-related-potentials (ERPs) were recorded for various behavioral events occurring during the task (Figure 3.2B). ERPs were established by thresholding and smoothing the firing rate from any single units detected. A snap-shot of the firing rate was averaged over behavioral features, such as entering/exiting any target and initiation of movement. The majority of sites showed no correlation.

Similarly to our SEP analysis, a heat map corresponding to the strength of response above baseline, visualized electrode sites dominated by correlated motor activity. If activity (Figure 3.2C) was detected such as excitation post-event, sustain during event or pre-event, these sites were excluded from possible selection for the experiment. electrodes with high (above 500 kOhms) or low (50 kOhms) impedance were also ruled out. We then chose a site corresponding with sensory activity with no motor activity.

3.2.7 *Task Training with Stimulation*

Once animals completed their initial recording sessions, they were retrained to perform the task with stimulation cues instead of the light cues **[59, steps 17-23]**. A baseline stimulation pattern was substituted for the single light cue. This training allowed the animals time to become familiar with the stimulation. Since the stimulation is presented as only feedback to the joystick manipulation, we could see if the stimulation evoked visible movements. If so, a different electrode site was chosen.

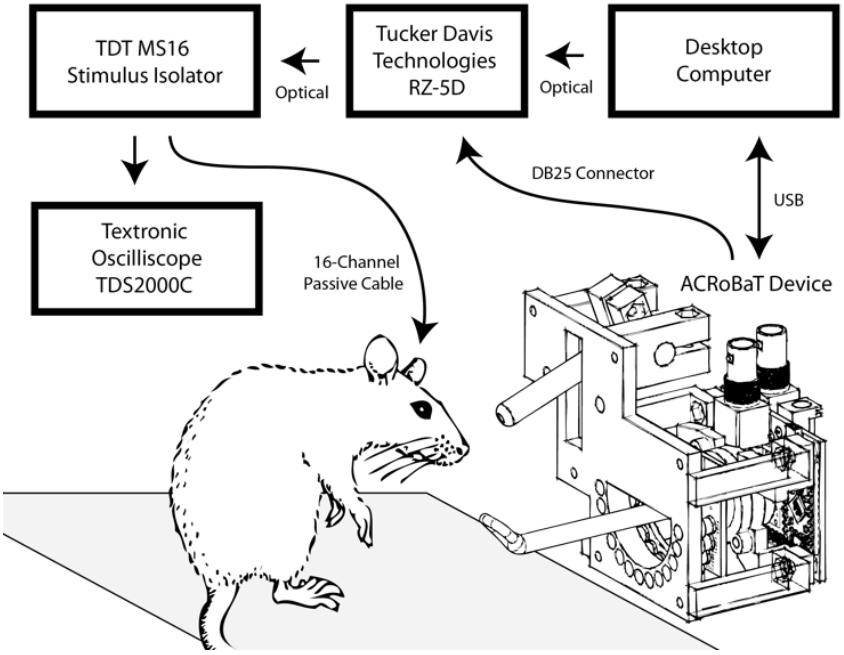

Figure 3.3. Experimental Setup

Measured behavioral actions and sensory stimulation were connected using the ACROBAT system. A desktop computer provided session parameters and the training/testing level via USB to the ACRoBaT onboard microprocessor. The ACRoBaT system ran the session as the master, returning behavioral variables to the desktop computer for logging. The Tucker Davis Technologies (TDT) RZ-5 responded as a slave module, read stimulation values via a custom serial protocol. The TDT MS16 Stimulus Isolator, linked via an optical cable, generated a stimulation waveform based from parameters, and delivered it to the implant. An oscilloscope was placed in parallel with the implant to monitor for any changes in impedance.

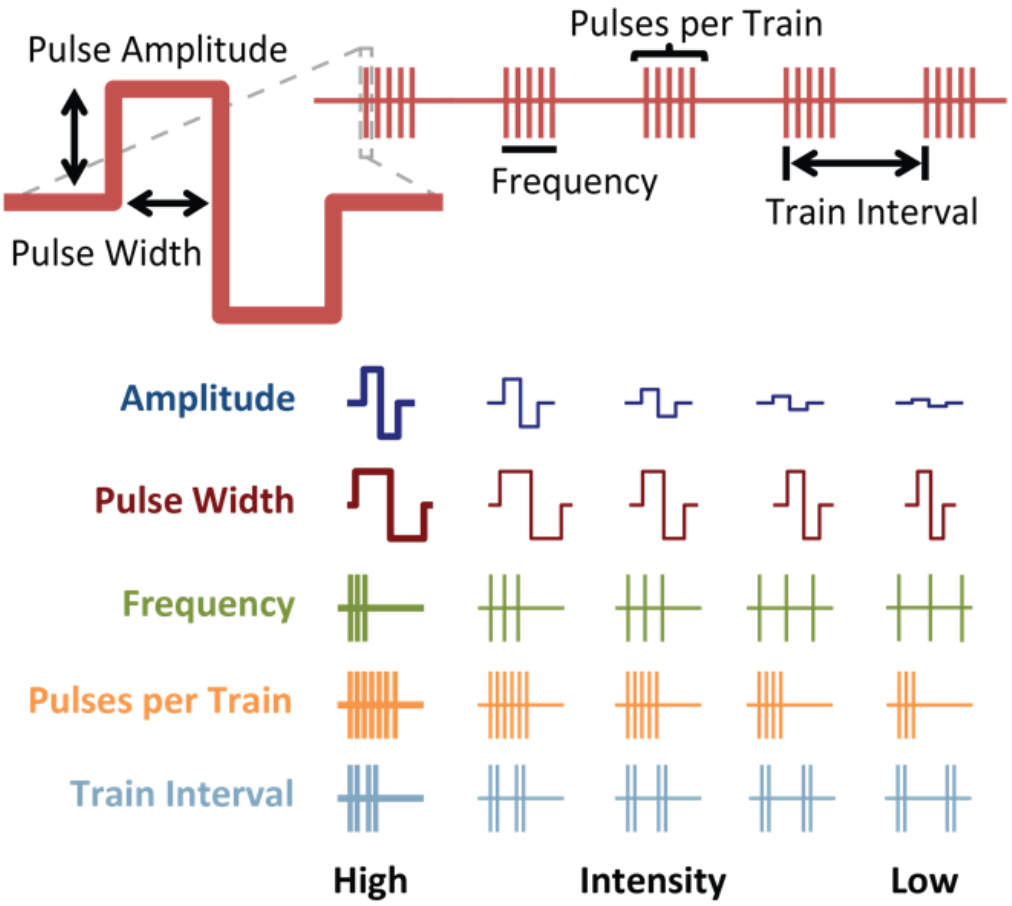

Figure 3.4. Stimulation Parameters

TOP: Five stimulation parameters were explored, modulated independently to measure the cortical sensitivity. Each stimulation pulse was constant current, bi-phasic and symmetrical. Amplitude refers to the height of each pulse phase, and pulse width the width of each phase. Frequency is the time between each pulse in a single train. Pulses per Train is the number of pulses in each train. Train Interval is the time between the start of each train.

BOTTOM: These parameters could be varied individually or concurrently. These graded signals were presented such that higher amperage, longer pulse width, higher frequency, greater number of pulses and shorter train intervals corresponded to higher intensity. Animals were trained to distinguish between a single higher intensity pattern, and randomly presented lower intensity patterns.

3.2.8 *Experimental Setup*

Our behavioral data collection system (Figure 3.3) integrated data from several sources, synchronizing training variables, stimulation parameters and real-time output to the implant. The ACRoBaT system was the master, passing behavioral variables to the desktop computer for logging, sending updated stimulation parameters to the Tucker-Davis Techniques (TDT) benchtop neural interface, RZ-5. Initial training level parameters were sent by a GUI on the desktop computer, determined session parameters and the training/testing level on the ACRoBaT onboard microprocessor. A custom serial protocol allowed the TDT RZ-5 to read stimulation values from a DB25 parallel cable connected to the ACRoBaT. A 16 channel passive cable connected the stimulator to the implanted array on the animals' head and allowed it to freely move around the arena.

3.2.9 *Stimulation Parameters*

We defined a set of 5 features to describe our stimulation paradigm, amplitude, pulse width, pulse frequency, train interval, and number of pulses based on those commonly used in the literature (refs) (Figure 3.4). The base stimulation pattern had an amplitude of 70µA, pulse-width of 200ms, train interval of 100ms, pulse frequency of 300Hz, and five pulses per train.

We defined corresponding ranges of each of these parameters for both safety (Merrill, Bikson, & Jefferys, 2005; Rajan et al., 2015; Shannon, 1992) and ability to recruit cortical neural populations. **Amplitude** defines the height of each pulse, within a range from 5 – 120µA. **Pulse Width** defines the width of each pulse, within a range from 50 – 500µs. **Frequency** defines the rate of each stimulus pulse within a train , within a range from 50-400Hz. **Pulse per Train** defines the length of a stimulation train (range of 5-20 pulses per train) and the **Train Interval** defines the time between stimulation trains (varying from 50 - 400ms).

Several other parameters remained fixed throughout all the experiments, including requirements that pulses are bi-phasic (mirrored) and constant-current. Thus, we could prevent the charge build-up around the electrode tip from damaging the surrounding tissue (Merrill et al., 2005; Rajan et al., 2015; Shannon, 1992).

3.2.10 *Parameter Range Detection*

The final step was determining the lower perceptual threshold of some parameters, specifically, the lowest possible amplitude which the animal could perceive. A basic detection task between a base stimulation pattern and a zero-amplitude pattern, determined the lowest possible perceived amplitude and pulse-width value. Animals could perceive any value in the range for the other parameters.

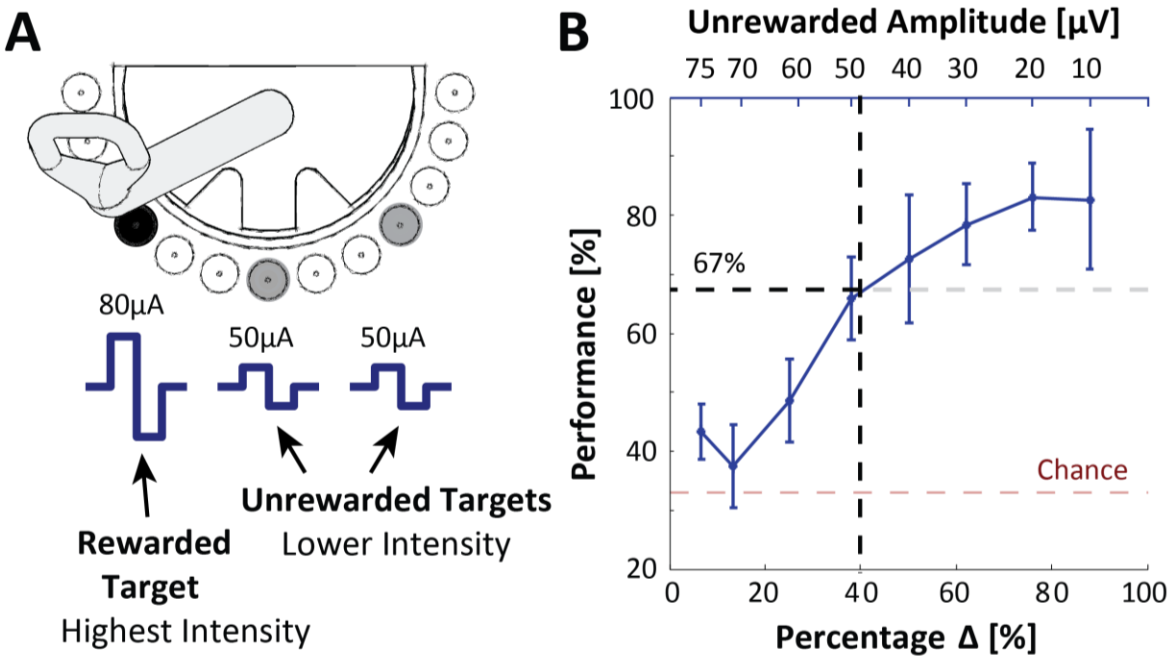

Figure 3.5. Just-Noticeable-Differences

Part A: A three alternative forced-choice task was used to assess discriminability. A high intensity parameter value (such as 80 µA) was chosen as the rewarded answer, while a variety of lower intensity parameters (70, 60, 50, 40, 30 µA, etc) were presented as unrewarded answers. The rewarded target was randomly chosen for each trial, and both the other targets randomly assigned the same lower intensity value.

Part B: Discriminability is plotted as the performance of identifying the high intensity parameter vs the lower value distractor targets. In this example, when the difference between the rewarded parameter and the unrewarded parameter is greater than 30 µA, the animal was able to correctly identify the higher value parameter more than 67% of the time. Chance for a three choice task is 33%.

3.2.11 *Just-Noticeable-Differences*

To reliably compare the resolution of each parameter, the Just-Noticeable-Difference (JNDs) was explicitly measured. The JND measurement is the magnitude of change required for the animal to detect a difference between two signals. By using this method to determine resolution of a signal, each pattern was modulated until the animal could reliably discriminate between the rewarded pattern and the unrewarded patterns.

For simplicity, the rewarded pattern was nominally a “higher intensity” pattern, corresponding to higher amplitude, longer pulse width, shorter train intervals, higher pulses-per-train, and higher pulse frequency (Figure 3.4). Unrewarded patterns were “lower intensity” corresponding to lower amplitudes, shorter pulse-widths, longer train-intervals, fewer pulses-per-train, and lower pulse frequency.

We used a forced three choice task to measure discriminability (Figure 3.5A). During a single session, a high intensity parameter value (such as 80 µA) was chosen as the rewarded pattern, while a variety of lower intensity parameters (70, 60, 50, 40, 30 µA, etc.) were presented randomly as the unrewarded patterns. In this example (Figure 3.5B), we see the animal can significantly distinguish between the two delivered intensities when the difference between the rewarded amplitude and the unrewarded amplitude is greater than 30µA. We can also see this threshold value can be expressed as a percentage difference between the two amplitudes (Figure 3.5C). In this example, a 40% change in amplitude is required for the animal to discriminate between two delivered sensations.

To control for learning effects, the location of the rewarded target was randomized trial by trial; while the rewarded pattern was constant throughout each session. The unrewarded patterns also varied trial to trial. Locations of the two unrewarded and single rewarded pattern

was randomized by trial (Figure 3.5A). A psychometric curve was fit based on the percentage correct (Figure 3.5B). Since this was a three-alternative forced choice task, our chance percentage level was 33%. The sensory threshold is nominally (Smith, 2009) set halfway between chance (33%) and 100%, resulting in a threshold of 67%.

Technically, only a two target task was needed for these discrimination task, however; a three choice task was preferable given the tendency for the animals repeatedly visit only one target. In order encourage a more random search strategy, a 20 trial history was used to negatively bias the selection of the location of the reward target away from targets where the animal historically successfully accomplished the task. This adaptive algorithm was highly successful in preventing repetitive movements to a single target location.

3.3 RESULTS

Towards our goal of developing a high-resolution sensory feedback signal delivered via electrical stimulation to the sensorimotor cortex, we measured the resolution of many types of graded stimulation encodings in the same animal and at same electrode site.

3.3.1 *SEPs and ERPs*

In each animal (Figure 3.6), we measured sensory evoked potentials (SEPs) and event related potentials (ERPs) to verify final electrode location with a cortical region targeted. Heat maps (Figure 3.2B,D) from a single animal with corresponding recorded signals (Figure 3.2A,C) were built to map electrode sites to either sensory or motor networks. We could then easily identify candidate electrode sites for our experiment, and eliminate those in the near vicinity of motor neurons.

3.3.2 *Just-Noticeable-Differences*

We recorded just-noticeable-difference (JND) measurements of a variety of stimulation encoding paradigms, allowing us to explore the resolution across the full range of delivered intensity. Using a three alternative force-choice task, we could assess each animals' discriminability between a high intensity sensation and lower intensity sensations (Figure 3.5A). We began our exploration by modulating intensity by varying a single stimulation parameter, and fixing all others to nominal perceivable values (Figure 3.4).

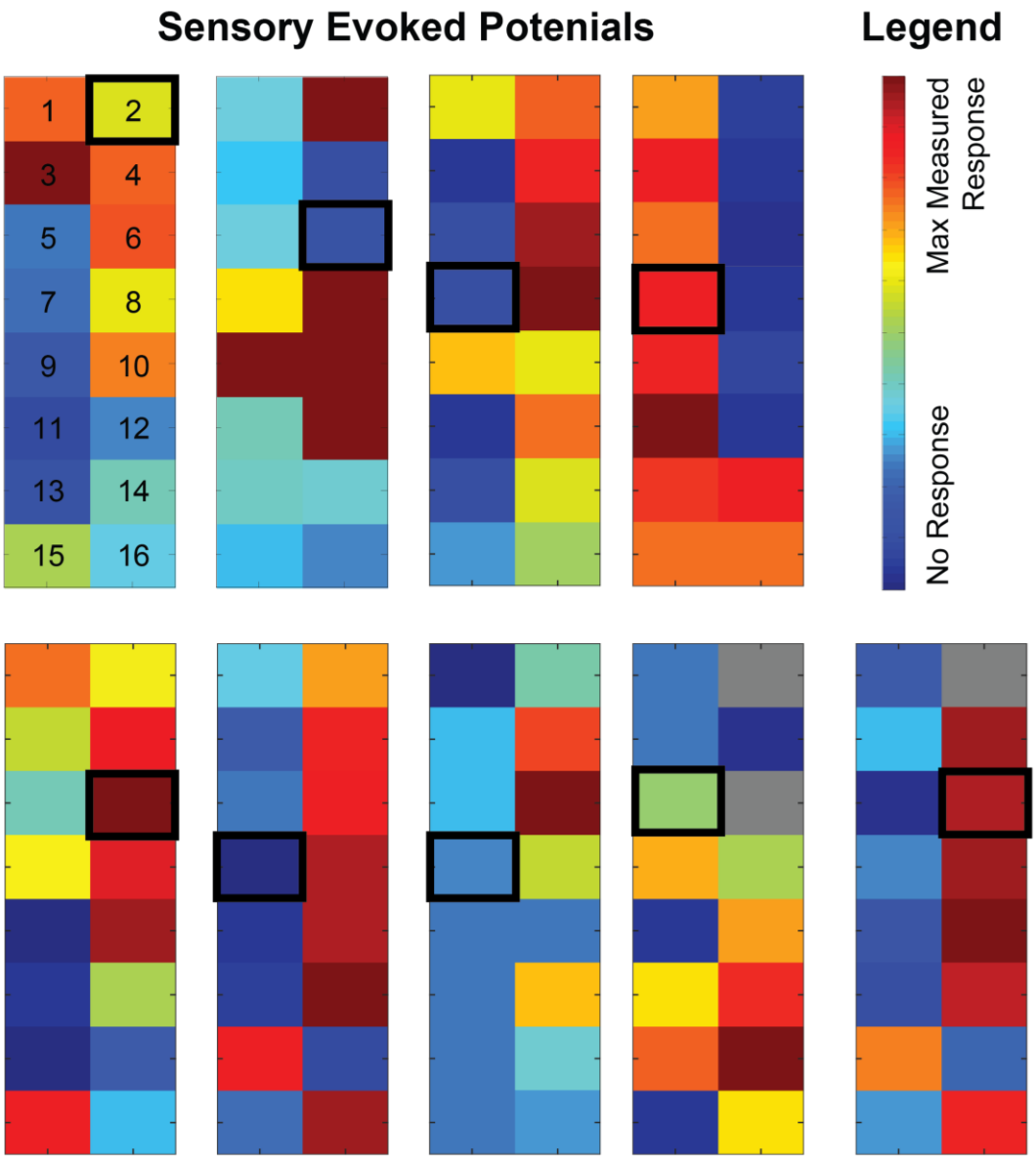

Figure 3.6. SEP Measurements for all subjects

Sensory evoked potential heat maps for each subject. Channels are numbered as found on the first example, and black outlined boxes indicate the electrode selected for sensory feedback. Grey boxes were channels excluded due to poor impedance measurements.

We plot discriminability as the performance of identifying the high intensity rewarded sensation vs the lower intensity unrewarded sensation (Figure 3.5B). Since our goal was to capture the JND resolution across the entire range of perceivable intensities, we repeated the form of the experiment several times, each with a different rewarded “high intensity” value (Figure 3.7A). Here, we plot the overlaid psychometric curves when the high intensity parameter was amplitude, and ranged from 40 - 80µA.

3.3.3 *Normalization*

To measure the resolution at the low, middle and high end of the intensity scale, we collected several different JND measurements, each with different rewarded “high intensity” pattern. Since each parameter had a different magnitude from min to max value (Figure 3.4), and in order to directly compare paradigms, we normalized each parameter range as a function of percent change (Figure 3.7B,E).

We plot a range of psychometric curves for a variety of amplitudes and pulse-widths as an example in Figure 3.7A and D. Normalized psychometric curves are generated by plotting amplitude and pulse width as a function of the percentage of the rewarded parameter value. For each animal, these individual psychometric curves were fit by a single sigmoidal curve (Figure 3.7C, F) for comparison across animals (Figure 3.8). Weber Fractions, calculated as percentage change required to cross the sensory threshold line (67%), were used to compare sensitivity across parameters and animals.

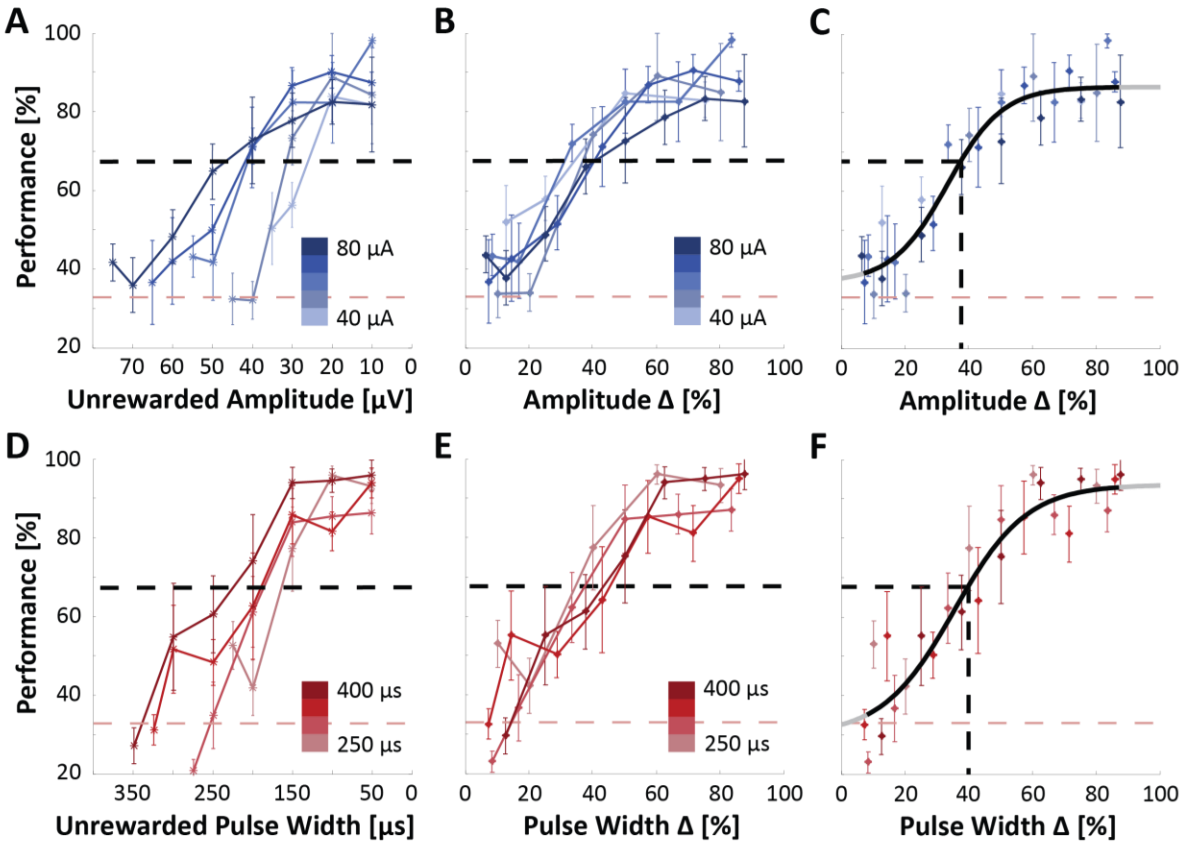

Figure 3.7. Normalizing JND measurements across a parameter range

Psychometric curves showing performance of discrimination between the rewarded "high intensity" pattern (shown in the legends) vs the unrewarded value (plotted on the x axis). On average 50 to 100 trials were collected for each individual data point.

Part A: We measured individual psychometric curves throughout the perceivable range of stimulus amplitude. Here, we show an example of five curves collected when the rewarded intensity value ranged from 40 - 80 µA. Within a single session, this highest intensity rewarded value was fixed.

Part B: The same data is plotted, but normalized such that the x axis shows the percentage difference between the rewarded amplitude value and the unrewarded amplitude value. For

example, if the rewarded value was 80 µA, and the unrewarded amplitude was 30 µA, normalization would set the percentage difference at 62.5% ((80µA - 30µA) / 80 µA = 0.625).

Part C: All the data points are used to fit a sigmoidal curve, which accurately describes the data. These psychometric curves are calculated individually for each animal. The Weber Fraction is calculated as the point which this sigmoidal curve crosses the sensory threshold, 67%.

Part D,E,F: An example of the same process is repeated for the parameter pulse-width. Note the similarities between Parts C and F. These fitted curves significantly overlap for each animal.

3.3.4 *Single Parameter*

We show all the fitted sigmoidal curves for each animal tested (Figure 3.8) and used the fitted sigmoidal curves to compare measured resolution across animals. The highest resolution parameters pulse-width (n=5) and amplitude (n=8) measured weber fractions of 0.30±0.03 and 0.34±0.06, respectively. This means, on average, an approximately 30% change in either parameter is required for the animal to reliably recognize two patterns as distinct. These were the lowest single parameter JND measured. Interestingly, for both amplitude and pulse-width, each of these individual psychometric curves significantly overlapped when normalized.

The measured resolution when modulating frequency was surprisingly inconsistent (Figure 3.8D), measuring a weber fraction of 0.86±0.07. Three out six of our animals tested were unable to discriminate between even the highest (400Hz) and lowest (50Hz) values of our range. One animal showed only moderate success at frequency discrimination, measuring a 0.60 weber fraction, meaning a 60% change in frequency was required to discriminate different frequencies (Figure 3.8D). When plotting the same data by unrewarded frequencies (Figure 3.11A), the only comparisons that cross the sensory threshold occur when one of the comparison frequencies is at or below 100Hz. Our conclusion is that lower frequencies may be discriminable, but performance declines when higher frequencies are used.

Measurements of resolution for train interval showed moderate, but consistent, sensitivity. The measured weber fractions hovered around 0.65±0.07. This meant a 65% change in the train interval was required to reliably discriminate between the “higher intensity” rewarded train and the “lower intensity” unrewarded trains. We also measured the minimum time interval required for the animal to discriminate between pulses delivered as continuous tonic stimulation, and pulses delivered grouped as pulse trains (Figure 3.8E, dotted line). This experiment showed

pulse trains occurring at a rate of faster than 100ms per train were perceived as tonic, continuous stimulation, setting a lower bound for delivery of distinct pulse trains. Thus, modulation of train interval is a reliable way to modulate intensity, but resolution is low. Therefore, there are few discriminable steps possible between the maximum and minimum of the tested range.

Modulation of the parameter pulses-per-train (ppt) required much more change to be perceived as a different intensity. The majority of our animals (6 out of 7), could not discriminate between the highest (20 pulses) and lowest (5 pulses) values of our range (Figure 3.8E). The only animal able to distinguish between the highest and lowest values did so when the experimental paradigm was reversed (Figure 3.8E, dotted line). This meant we rewarded the animal for the lower intensity sensation (5 ppt) discriminating between several higher unrewarded intensity values (10, 12, 15 20 ppt). On average, the amount of change required for the animal to reliably discriminate two patterns exceeds our range.

To compare across all parameters, we plotted average weber fractions and standard deviation in Figure 3.8A. Pulse-width and amplitude required the least percentage of change before the animal could significantly discriminate between the rewarded intensity and the unrewarded intensities. Temporal parameters such as train interval, frequency, and pulses per train demonstrated surprisingly low sensitivity during direct brain stimulation. Psychometric curves fitted with a sigmoid for each parameter show a clear trend: pulse-width and amplitude have the lowest JNDs, and thus the highest resolution encoding scheme.

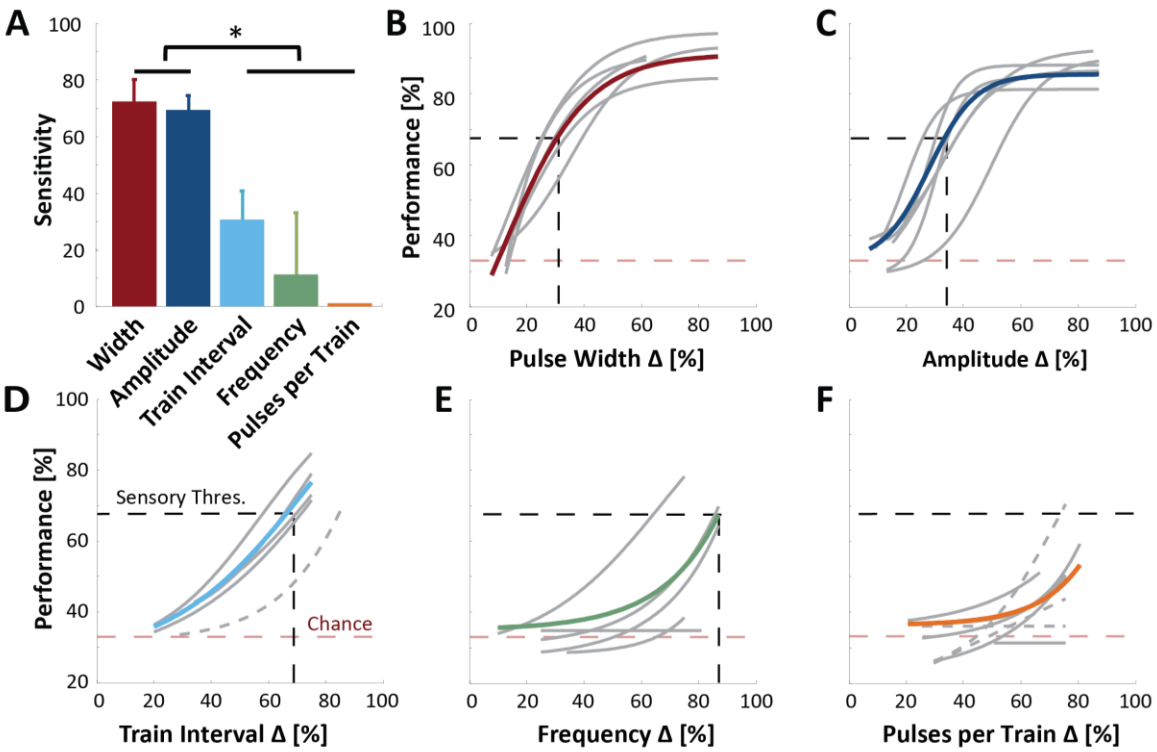

Figure 3.8. Single Parameter Sensitivity

Just-Noticeable-Difference (JND) curves for measuring the Weber fractions while modulating each parameter individually.

Part A: Weber fractions (WF) show which parameter has the lowest JND. WF's are calculated by the percentage required cross the sensory threshold (67%), and plotted as the inverse (sensitivity = 1-WF). Bars show data from colored sigmoid curves cross the sensory threshold, while error bars show standard deviation of where each grey line crosses the sensory threshold. Pulse Width has 2971 trials across 5 subjects, with 43±12 trials per data point. Amplitude has 6283 trials across 8 subjects, with 56±30 trials per data point. Train Interval has 1965 trials over 5 subjects, with average of 57±26 trials per data point. Frequency has 2174 trials across 6 subjects, with average 54±31 trials per data point. Pulse per Train had 2194 trials over 7 subjects with average 56±33 trials per data point.

Part B-F: A fitted sigmoid curve in color shows the average response across all animals. In grey, each animal's individual data is shown as a fitted sigmoidal curve. Dotted lines show data where the animal was asked to identify the lower intensity value. Pulses per train is the only parameter which never crosses the sensory threshold, thus its sensitivity score is 0. Y-axis shows percentage correct of trials and x-axis show the percent change between the rewarded higher intensity pattern and the unrewarded lower intensity patterns. The data shows amplitude and pulse-width modulation have the highest sensitivity to changes, while the other parameters require the magnitude of change to be two times or greater for the same discriminability performance.

3.3.5 *Charge-per-pulse (CPP)*

The discovery of the high sensitivity parameters amplitude and pulse-width led us to designed two follow up experiments to further disentangle the effects of modulating charge per pulse. We designed one graded stimulation paradigm, rewarding longer pulse-widths as the "higher intensity" value. Instead of fixing all other parameters however, we also co-modulated amplitude negatively such that the charge-per-pulse (CPP) remained constant across the entire range (Figure 3.9A). Specifically, the product of the two parameters pulse-width x amplitude was set to a constant value. When comparing this psychometric curve with single parameter modulation (see Figure 3.8C), the animal is no longer able to discriminate between any values in the encoded range (Figure 3.9A, black line). We repeated the experiment by rewarding the "higher intensity" pattern as larger amplitude values (Figure 3.9B). Here, the rewarded "high intensity" sensation was encoded as a short pulse-width, high amplitude pulse and the unrewarded "low intensity" values were a long pulse-width, low amplitude pulse (Figure 3.9B, black line). With charge-per-pulse held constant, the animal was unable to discriminate different amplitudes over nearly the entire range.

This evidence suggested the sensory cortex is really responding to the underlying variable, charge-per-pulse. From this line of reasoning, it should stand to suggest that modulating this variable directly would correspond to the highest JND, or highest resolution encoding scheme. We tested this hypothesis in Figure 8C and saw nearly a 50% improvement on the JND. When high intensity was encoded as a long pulse-width, high amplitude pulse and low intensity was encoded as a short pulse-width, low amplitude pulse (Figure 3.9C, purple line), only a 15% change was required for significant discriminability compared to nearly a 30% change required when amplitude or pulse-width were modulated individually.

In summary, we find the most discriminable parameters to be charge-per-pulse, pulse-width, and amplitude. These parameters require changes of only 15%, 30% and 34%, respectively in order to be discriminated as different (Figure 3.10A). Train interval is also a reliable parameter, but requires a 65% change to be detected as different. Frequency is an unreliable parameter to modulate in order to convey sensory information, as half of our animals were unable to interpret any change in frequency when the charge-per-time is carefully controlled. Modulating pulse-per-train also seemed to have little effect on perception, possibly due to the small number of events (5-20 pulses) and the short intervals per train.

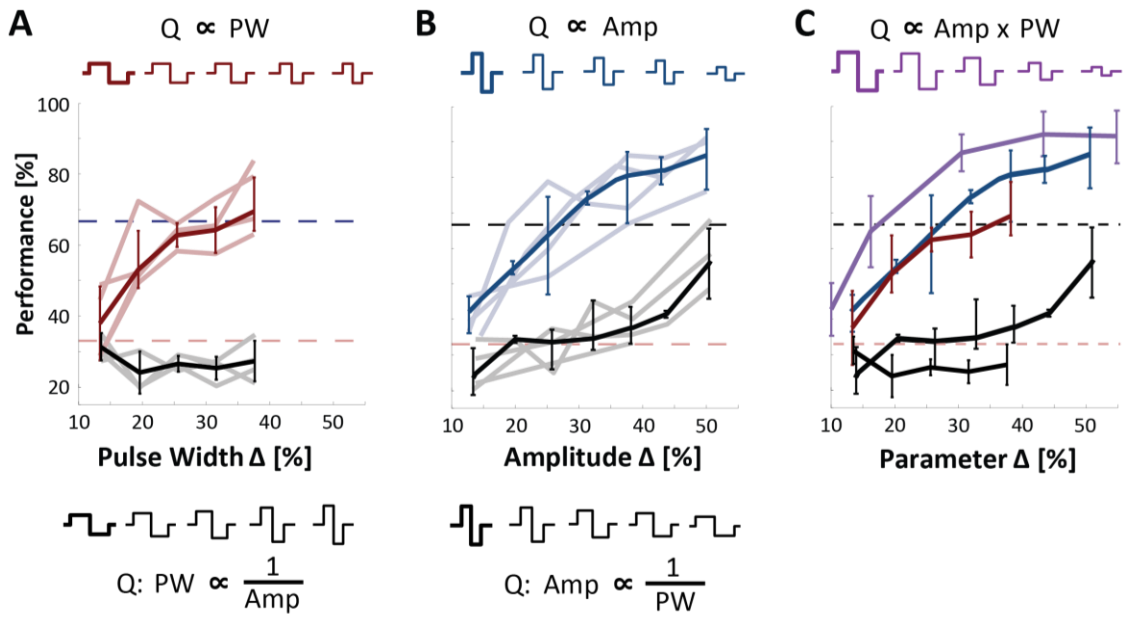

Figure 3.9. Charge Per Pulse Sensitivity

To explore the effects of charge per pulse (CPP) we varied amplitude and pulse-width inversely, constraining the charge per pulse to be equal.

Part A: In the black, we varied pulse-width negatively and amplitude positively such that the rewarded pattern had a wide pulse-width and small amplitude. Unrewarded patterns had a shorter pulse-widths and higher amplitudes such that the charge, or area under the curve, was constrained. 3365 trials were recorded across 5 subjects.

Part B: In the black, we modulated amplitude negatively and pulse-width positively. The rewarded pattern had high amplitude and short pulse-width, while the unrewarded patterns had lower amplitudes and longer pulse-widths. We recorded 2316 trials across 4 subjects.

Part C: Here we combine amplitude and pulse-width positively. As expected, we see a significant boost in sensitivity. Shown in purple, this psychometric curve crosses the sensory threshold at 15%. Total trial count was 5926 across all conditions and 5 subjects.

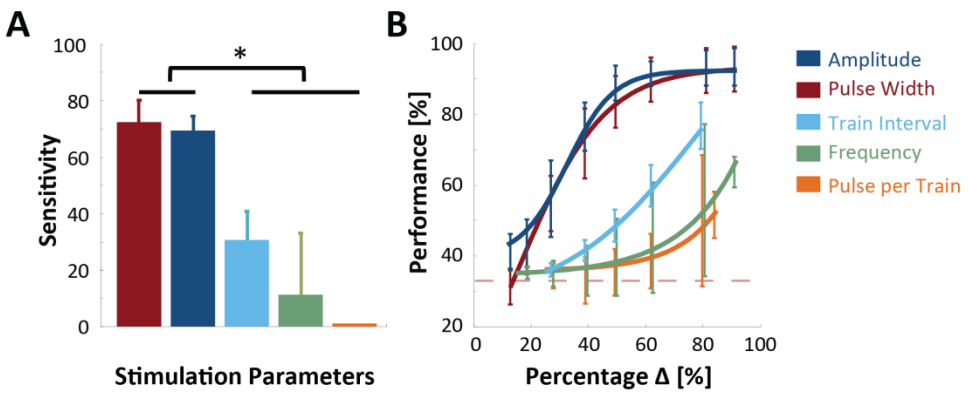

Figure 3.10. Final Results

Overlaid psychometric curves for each parameter tested, averaged across all animals.

Part A: Bar graphs show average Weber Fraction values when psychometric curves crossed the sensory threshold (67%) and error bars show standard error of the mean across animals.

Part B: Psychometric curves for each parameter. Error bars show max/min spread of values measured. Pulse width and amplitude dominate the sensitivity measures while train interval is reliable but weak. Frequency is unreliably detected by the animals, as is varying the number of pulses-per-train.

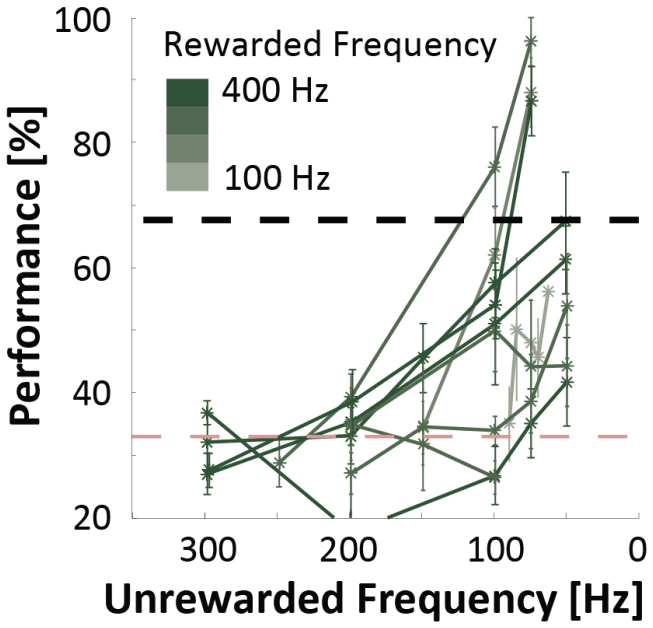

Figure 3.11. Frequency Discrimination

Individual psychometric curves for all of the animals tested (n=6). No significant discrimination is measured between two pairs of frequencies unless one of the pairs is less than 100Hz. The x axis displays the unrewarded frequencies, while the legend indicates the rewarded frequency. Each curve is a single rewarded frequency.

3.4 DISCUSSION

Our experimental goal was to understand which types of sensory encoding schemes are easily understood by the brain and which ones are more challenging. Our experiments clearly demonstrate that modulating either amplitude or pulse-width requires only a 30% change to discriminate between two different stimuli. Modulating amplitude and pulse width concurrently is even more effective, requiring only a 15% change. These paradigms for encoding intensity require the least amount of change of all paradigms tested. This leads us to conclude the charge-per-pulse (CPP) is a primary variable for modulating artificial sensory perception.

3.4.1 *Unreliable Frequency Discrimination*

Surprisingly, we find discrimination between high frequency pulse trains to be an unreliable way to convey sensory feedback. Five out of six animals were either completely unable to discriminate between any two frequencies tested (n = 3) or only able to discriminate between the highest and lowest values in the range (n = 2). Other temporal parameters such as varying the train interval were only moderately perceptible, requiring a 65% change for reliable discrimination. Modulating the number of pulses per train was not perceptible to nearly all animals.

Our results must be rectified with previous work suggesting stimulation at discrimination between different frequencies is possible (Fridman et al., 2010; O'Doherty et al., 2011b; Ranulfo Romo et al., 2000; Thomson et al., 2013). These studies suggested that frequency discrimination was not only possible, but likely the most promising method for feedback. Given the historical emphasis on frequency modulation in the sensory stimulation literature, below we carefully compare our results to prior work.

Romo conducted experiments to measure discriminability between different low frequency (< 44Hz) ICMS and mechanical flutter stimuli applied to the fingertips. Primates were reliably able to substitute low frequency tonic ICMS with sensations caused by mechanical flutter stimuli (Hernandez, Zainos, & Romo, 2000, Figure 1d). A frequency range of 10Hz to 30Hz adequately mapped to the same range of mechanical stimuli. However, when asked to discriminate between two different low frequency ICMS patterns in the same range, the task became more difficult (Hernandez, Zainos, & Romo, 2000, Figure 5c, grey line). The primate could discriminate between 20Hz and 30Hz, but this represents a 50% difference in frequency. In addition, significant time is required to communicate using a train of low frequency pulses, which could significantly limit the bandwidth of artificial sensory feedback.

A brain-machine-brain interface (BMBI) provided direct cortical feedback in response to exploration of a three target workspace (O'Doherty et al., 2011b). Primates were rewarded for discriminating between two different frequencies of stimulation and a third target with no stimulation. This successful demonstration of interleaved decoding motor intent and delivering sensory feedback indicated primates might be able to discriminate between 200Hz vs. 400Hz stimulation. The different stimulation trains were carefully designed to interleave with recording blocks, and deliver the same amount of total charge over a 500ms window. This meant that frequency was not the only parameter modulated. When frequency doubled over the same train length, the number of pulses also doubled, and the train-interval doubled as well. Our data suggest that animals in this study may have cued on the change in train-interval, perhaps more so than the change between the two high frequency trains.

In another study by the same group, rats chose from one of three water ports based on the frequency of electrical stimulation delivered to the whisker representation of S1 (Thomson et al.,

2013). Stimulation was delivered in a continuous train with frequency proportional to their orientation towards the correct target, and a maximum rate of 300Hz. These rats performed the task well when the ports were located at disparate locations throughout the circular arena. However, when the ports were closer than 60 degrees from each other, the animals' performance significantly dropped. Although the paper does not provide the exact mapping from target location to stimulation frequency, based on our results, we predict that frequency dropped below 100Hz when the animal was facing more than 60 degrees from the correct port. The charge per time delivered to the cortex significantly changes between 300Hz and 100Hz. We believe this would permit the discrimination of very low frequencies as we have seen possible in our data.

Separate experiments in the non-human primate measured the just-noticeable-difference (JND) of different amplitudes of stimulation (Kim et al., 2015). The authors explored different pulse-widths, frequencies and pulse train lengths while they tested for stimulus amplitude discrimination. Therefore, data from this study permits an indirect examination of the effects of frequency. Their results demonstrate no significant change in amplitude JNDs across a frequency range from 50Hz to 500Hz, suggesting the frequency component does not contribute to a perceived stimulus intensity (Kim et al., 2015, Figure 4B). Our data reinforce this interpretation since our animals were unable to discriminate between similar high frequency stimulation trains.

We carefully examined the data from our single animal that appeared to adequately discriminated frequency (Figure 3.11). The most likely explanation of higher performance in this animal is that the particular network activated was very sensitive to stimulation at 75Hz. This animal could reliably distinguish between 75Hz and nearly every other frequency, but was unable to discriminate between similar percentage differences higher in the frequency range. This observation suggests that rather than wide-spread ability to perform frequency

discrimination, this animal was reliably able to discriminate 75Hz stimulation from all other frequencies.

Given the prior work summarized above, combined with our current findings, we conclude that lower frequency discrimination may be possible for frequencies below approximately 100Hz. Performance significantly degrades, however, when using higher frequencies to convey sensory feedback. The inability to perform frequency discrimination when charge per time is fixed could be evidence of a fundamental upper limit on the brain's ability to discriminate between higher stimulus frequencies.

3.4.2 *Modeling of Neural Network Activation*

It would be advantageous to be able to accurately model the selective activation of sensory regions, and use it to explore the effects of electrical stimulation on perception. Given the high dimensional stimulation parameter space, computational models could reduce the substantial workload to experimentally test all stimulation conditions and their interactions. Two groups (Fridman et al., 2010; Kim et al., 2017) have developed limited models to explain the effects of their stimulation paradigms, but the field has yet to coalesce upon a verified model to explain the effects electrical stimulation.

Fridman *et al.* (2010) used a leaky integrator model of delivered charge to predict perceived intensity. They experimentally validated this model by selecting several fixed points in the stimulation parameter space (varying frequency, amplitude, and train duration). They estimated the parameters of the model through a threshold detection tasks, and it accurately predicted trained rodent behavior discriminating between several fixed points in the space. However, this model was fit with different parameters for each set of comparisons that varied along each dimension separately, making it difficult to generalize.

Kim *et al.* (2017) created a uniform model by building a population model of stimulated neurons. This model computed the probability of each neuron responding to 11 free parameters of ICMS train including previous firing history, distance from the electrode, and injected charge over time. Using an ideal observer analysis, the model was fit to predict behavioral response to a detection task and an amplitude discrimination task. This model performed well, but was not validated by discrimination tasks for any of the other parameters. Further work is required to computationally predict the sensory perceptual response to the wide variety of possible ICMS stimulation trains.

3.4.3 *Weber's Law*

Although our experiments were not designed to test Weber's hypothesis (Fechner, 1860), we see evidence that perceived intensity of ICMS may follow Weber's Law for amplitude and pulse-width modulation. Weber's Law predicts that perceived intensity will be proportional to the percent change of a stimulus, rather than an absolute unit of value (such as mico-volts). When normalizing to percent change of amplitude and pulse-width in Figure 3.7B,E, each resulting psychometric curve overlaps. Thus, Weber fractions are relatively constant despite the absolute change of more than 200% compared to the lowest value parameter.

3.4.4 *Implications for neural interface design*

The goals of our experiments were to both determine the resolution and to maximize the band-width of the delivered stimulation parameters. Given that most BCI technology uses visual feedback as the primary mechanism for guiding control strategies, our ICMS feedback patterns were designed to improve on the slow visual feedback pathway (~200 ms delay). Therefore, we explored relatively short train-intervals (our nominal value was 100 ms) and a small number of

pulses-per-train (<20). In comparison, others who have studied electrical stimulation have used relatively long pulse trains (200 – 1000 ms) and a large number of pulses (>50-100 pulses per train) (Fitzsimmons et al., 2007; Fridman et al., 2010; Houweling & Brecht, 2008; R Romo et al., 1998). These differences in stimulus train length may also help to explain the differences between our results and previous studies. We emphasize, however, that using longer pulse trains may compromise the temporal resolution of conveying rapid sensory feedback, especially in real-time neural interface applications.

Direct comparison of stimulation parameters in the same animal and brain region can be challenging. Using a rodent model and high-throughput behavior task (Bjånes & Moritz, 2018), here we could test these encodings in the same cortical circuit of each animal across nine different animals. This allowed us to collect thousands of trials to robustly compare the sensory discrimination of different parameters. Although differences in stimulus perception may exist between the rodent brain and primate brain, our results provide a strong foundation for testing promising sensory encoding schemes in non-human primates and human subjects going forward.

3.5 CONCLUSION

In conclusion, we have made significant progress towards our goal of developing a high-resolution sensory feedback signal delivered via electrical stimulation to the sensorimotor cortex. By measuring the resolution of many types of graded stimulation encodings in the same animal and at the same electrode site, we found that animals were most sensitive to changes in the parameters amplitude and pulse-width, which modulate the charge of the delivered pulses. Surprisingly, animals showed little sensitivity to modulation of higher frequency pulse trains. Finally, animals were able to detect train-interval but not the number of pulses in the train.

By determining which features canimals can detect during artificial stimulation, we can now design stimulation patterns to maximize resolution of an input signal. With the goal of delivering high bandwidth information directly to the brain, we validated stimulation parameters which could be updated and interpreted quickly. We recommend using the parameters amplitude and pulse-width to modulate intensity of a given percept (Figure 3.9C, purple line). Since the mechanism of network activation seems very similar, we next recommend modulating train interval if further input range is needed, although future experiments are required to determine orthogonality of these parameters. Our results provide insight into the optimal ways to provide feedback in a bi-directional brain computer interface, and help establish a platform for design of efficient electrical stimulation for sensory perception.

Chapter 4. FUTURE DIRECTIONS

The research discussed above presents many new exciting possibilities for future experiments and raises many new questions. One of the most exciting avenues for future exploration is human subject testing of the effects of each of these stimuli on perceived intensity. While the rodent model enabled us to gather a large data set and explore the parameter space thoroughly, these experiments were designed with translation in mind.

4.1 HUMAN ECOG EXPERIMENTS

Collaborations with colleagues at UW working with intractable epilepsy patients (Collins et al., 2017; Johnson et al., 2013) gave us an opportunity to share our findings about charge-per-pulse in a targeted set of experiments. During the planning and execution of the experiments performed in Chapter 3, ongoing discussions cross-pollinated both the experiments in the human trials, and provided us valuable feedback of potential avenues to explore in the rodent model.

4.1.1 *Discussion of slow reaction times to stimulation*

Data collected from human subjects regarding slow reaction times in response to visual, tactile and ECoG stimulation (Caldwell et al., 2017) was particularly intriguing. Confirming findings shown in Pittsburgh (Godlove, Whaite, & Batista, 2014) in healthy subjects and primates, reaction times were measured in response to perceived onset of ECoG stimulation, tactile stimulation and visual stimuli. Surprisingly, reaction times for the electrical stimulation was the slowest, potentially making it more difficult to establish a fast, low-latency pathway for motor-sensory tasks. Batistia's group found similar results using a *redirect task* instead of the *pressured reaction time task* employed by Ojemann's group. The redirect task more accurately

mimics motor feedback pathway during an ongoing motor task, rather than an attention specific initiation of a reaching motion.

There are a few explanations for why the reaction times to direct brain stimulation may be slower than natural sensation. First, the stimulation does not mimic a known sensation. Extra processing time may be required for the brain to isolate the input, determine the signal isn't noise, and integrate it with other sensory modalities. Second, the stimulation signal may need 'amplification' by downstream cortical networks; ICMS indiscriminately activates inhibitors and excitatory pathways. By only recruiting a neurons and axons nearby the electrode tip, conscious perception of the stimulus may take time to emerge, in contrast with a signal arriving through natural sensory pathways from the periphery. And thirdly, ICMS may activate particular brain regions out of the natural order. Ascending sensory information pathways are the expected route for the brain, and if areas 1, 2, or 3b are activated without their downstream partners such as thamlus or spinal cord afferent pathways, it may take time to recognize the signal.

Further experiments might isolate the cause for the increased reaction times. We would like to design an study to activate sensory signals at various points along the processing stream (first cutaneous receptors in the skin, then in the ulnar or radian nerves in the periphery, then thamlus, concluding all the way to the location activated in S1). By measuring reaction times associated with each of these downstream locations, we may be able to pinpoint the source of the delays.

4.1.2 *Aperture matching task*

Rao's group performed an interesting experiment requiring the subject to use three different frequency stimulation patterns to match a particular aperture of the hand (Cronin et al., 2016). Subjects were fitted with an instrumented glove, measuring how far they "opened" or

“closed” their hand. Three levels of stimulation (No Stim, Low Amp Stim and High Amp Stim) were given as feedback to match a sinusoidal trajectory, opening and closing the hand at a particular slow frequency (0.02Hz). Participants could not see the trajectory; they were instructed to close their hand if they felt the higher amplitude and open their hand if they felt the lower stimulation sensation. If they felt nothing, their hand was at the correct aperture. One participant was able to perform the task quite well, while another had lower, but significant performance. The stimulation was applied in 200ms trains, thus higher amplitude delivered more current per time, aligning with our theories on sensitivity to charge injected.

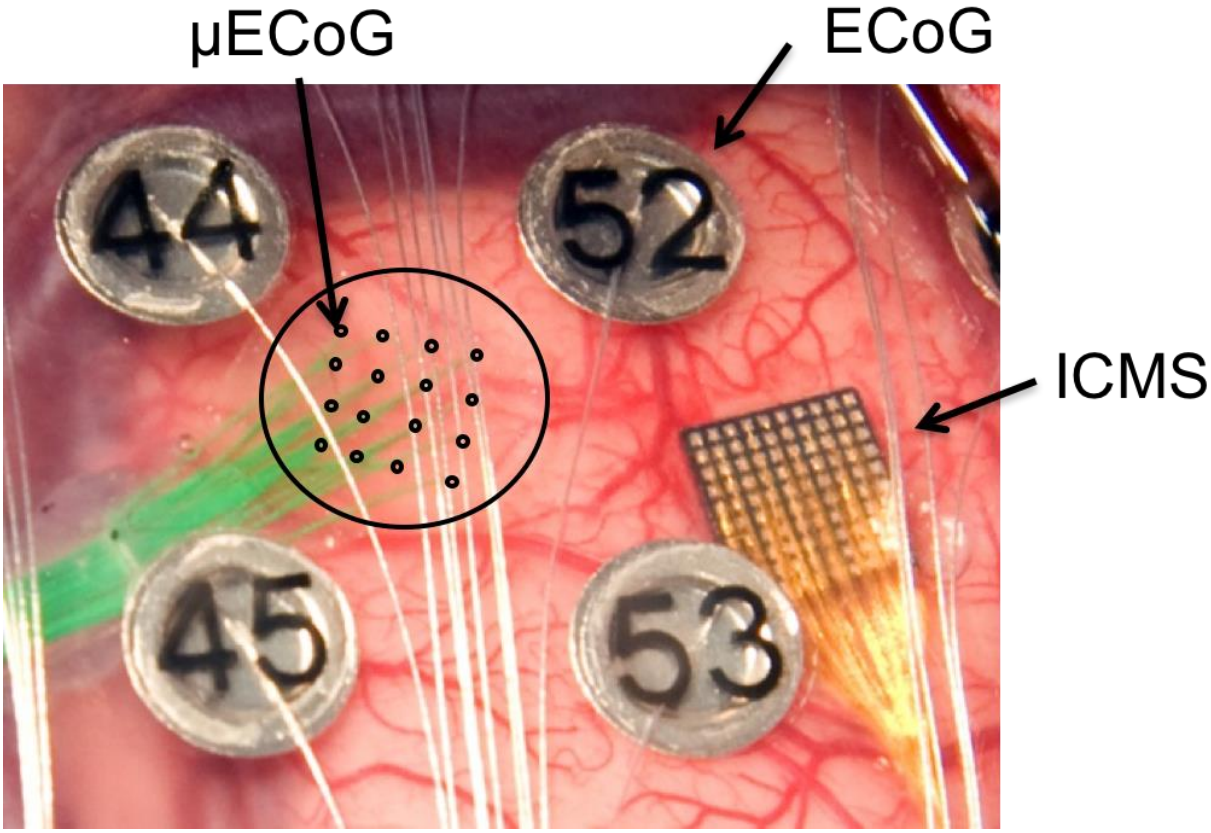

Figure 4.1. Final ElectroCorticoGraphy grids (ECoG)

Comparison of size among penetrating micro-wires (ICMS), micro-ECoG grids (µECoG), and standard clinical 'ECoG' arrays in a human brain. Background image from (Kellis, House, Thomson, Brown, & Greger, 2009).

4.2 Micro-ECoG Stimulation vs ICMS

Since our results in Chapters 2, 3 were measured using penetrating micro-wire technology, and the human experiments used standard clinical ECoG grids (Figure 4.1), we laid the groundwork for direct comparison of ICMS and micro-ECoG sensory stimulation. We co-authored a paper (Goshi et al., 2018) with our CNT partners at SDSU, testing recording and stimulation through novel µECoG grids fabricated with glassy carbon (GC) technology. Several animals were implanted and sensory-evoked-potentials were recorded, confirming accurate recordings through the interfaces. We also entered one animal into our behavioral training protocol and it was successful in using the stimulation delivered through the µECoG grid to complete the base task.

While macro ECoG arrays activate order of magnitude larger numbers of neurons, µECoG and ICMS wires are similar sized. Thus the comparison between them would be about the location of the stimulus (surface of the brain vs depth). We would expect the µECoG arrays have worse performance with temporal features, but it would be exciting to see if the spatial features had similar sensitivity. µECoG grids are FDA approved for a variety of conditions and implanted in thousands of people today. If future animal experiments showed that cortical sensitivity through µECoG grids was high enough, a large clinical population could potentially benefit.

4.3 Scalability of Interface (Multi-Channel Stimulation)

Another wide open question is the scalability of such an interface. All our experiments consisted of stimulation on a single electrode, conveying a single perception of intensity. However, when think about implementing our new found knowledge in a BBCI, there are

hundreds, if not thousands, of possible sensory channels which are integrated at a low level, but still accessible to varying degrees based on active user attention.

It does not seem possible that such a large number of sensory inputs could be consciously monitored or even perceived; certainly we are largely unaware of the deluge of incoming sensory information available to us on a moment by moment basis. Yet, our sensory processing system still has access to each one of these signals and promptly brings it to our attention when something is unpredicted or unexpected. Any well integrated artificial sensory system, in theory, should be able to provide access to a rich input of sensory data on command. Do we need to provide hundreds of individual sensory channels for the sensory cortex to absorb? Or should we have an online computer decide which inputs are most important to send and multiplex those signals through a more limited interface?

More concretely, as a sensory stimulation community, we have yet to address some fundamental questions. Is there a limit of individual channels which are distinguishable from each other (using electrical stimulation)? Are their diminishing returns to the amount of information available as the channels scale higher (i.e. 100% bandwidth is possible on a single channel, but two channels simultaneously might only have 50% bandwidth each, 4 channels – 25% each, etc).

It is also possible that higher level sensory perceptions maybe be required for full integration. Rather than send individual information regarding pressure or stretch at very local positions on a limb, we will need to send the state of the entire limb: where is the limb in space, what it the temperature, where is painful, etc. These higher level cognitive processes might lead us to interface with other regions of the brain rather than just S1, areas 1,2, or 3b.

4.4 Other Parameters

We have carefully built a framework allowing us to describe nearly all stimulation patterns currently found in the literature, with five basic parameters. However, these parameters assume a static temporal component which is unlike many signals recorded in the nervous system. Future studies should also consider using additional parameters for non-linear or time-varying components to more accurately mimic recorded signals.

Chapter 5. CONCLUSION

Somatosensation is an integral part of how each one of us interacts with our environment, explores and manipulates objects around us, and connects with the people we know and love. It helps us perform daily mundane tasks without spending much cognitive effort and gives us the necessary feedback to master difficult dexterous tasks like throwing a baseball or playing a music instrument. For patients who have suffered stroke or spinal cord injury and have significant impairment of somatosensation in areas of their body, quality of life can be severely impacted. Loss of sensation of their bladder and/or bowl, lack of painful stimuli, proprioception and cutaneous sensations can be dangerous, requiring constant vigilance, and full-time help with daily activities. For many of these people, a direct brain interface could restore sensations through direct stimulation of the sensory cortex, improving quality of life. For patients using a BCI to control external systems re-animate their own limbs, sensory feedback could improve control by sending high-resolution feedback from the limb directly to the brain.

5.1 High-Resolution Sensory Feedback Signal

This thesis has investigated parameters for evoking sensory perceptions via electrical stimulation of the sensorimotor cortex. We have identified the resolution of five encoding patterns, and tested animals' ability to utilize this sensory feedback to complete a motor task. We individually tested each parameter in order to determine which features modulated perceived intensity. Using a novel behavioral task for rats as a measure of comprehension, we measured psychometric curves to calculate the just-noticeable-differences of modulating each parameter defined in our stimulation framework. Given the factorial number of possible combinations of parameters and large ranges, we focused on testing combinations which could be updated and

interpreted quickly by the brain. These types of experiments allowed us to directly compare many possible high-bandwidth encoding paradigms. By comparing results in the same animal and same brain location, we demonstrated the brain was most sensitive to changes in amplitude and pulse-width. Surprisingly, animals were unable to discriminate between higher frequency stimulation. These results showed a lower-dimensional variable in the parameter space manifold; the charge-per-pulse of the electrical stimulation patterns yield the highest sensitivity measurements studied to date.

5.2 Novel Modified Center-out Task for Rodents

Several other milestones were accomplished during the experiments as well, including the development of automated, rapid training for a complex behavioral task for rats. The ACRoBaT device implements several strategies for significantly improving training times, and delivered a robust protocol free from human bias in monitoring or evaluating performance. With only a two to four week training requirement, our open-source platform lowers many entry barriers for complex behavioral research and can be used for a wide range of applications.

5.3 Micro-ECoG Device Development

We also helped the development of new technologies for epi-cortical stimulation of the brain, partnering with collaborators at SDSU. Our co-authored paper on the validation of novel µECoG devices manufactured with glassy-carbon material demonstrated improvement on the state of the art for both recording and electrical stimulation. These first steps are important for exciting new studies of the effects of brain surface stimulation through interfaces becoming more commonly used in human patients. We laid groundwork for future experiments with collaborators at the UW, working with intractable epilepsy patients, to translate our findings

from the rat model to human subjects regarding the perception of stimulation intensity as modulated by charge-per-phase.

5.4 Final Statements

In conclusion, we have made significant progress towards our goal of developing a high-resolution sensory feedback paradigm delivered via electrical stimulation to the sensorimotor cortex. Development of high-throughput automated training areas has lowered the barrier for rodent research exploring sensory stimulation of the brain. New epi-cortical stimulation devices can improve selectivity and advance the state-of-the-art beyond currently approved device for human patients. Our findings on stimulation encoding patterns provide insight into the optimal ways to provide feedback in a bi-directional brain computer interfaces, and help establish a platform for future design of efficient electrical stimulation of sensory cortical areas.

BIBLIOGRAPHY

Aflalo, T., Kellis, S., Klaes, C., Lee, B., Shi, Y., Pejsa, K., … Andersen, R. A. (2015). Neurophysiology. Decoding motor imagery from the posterior parietal cortex of a tetraplegic human. *Science (New York, N.Y.)*, *348*(6237), 906–910. https://doi.org/10.1126/science.aaa5417

Bachy-y-rita, P., Collins, C. C., Saunders, F. A., White, B., & Sscadden, L. (1969). Vision Substitution by Tactile Image Projection. *Nature*, *221*(5184), 963–964. https://doi.org/10.1038/221963a0

Bensmaia, S. J., & Miller, L. E. (2014). Restoring sensorimotor function through intracortical interfaces: progress and looming challenges. *Nature Reviews. Neuroscience*, *15*(5), 313–325. https://doi.org/10.1038/nrn3724

Berg, J. A., Dammann, J. F., Tenore, F. V., Tabot, G. A., Boback, J. L., Manfredi, L. R., … Bensmaia, S. J. (2013). Behavioral Demonstration of a Somatosensory Neuroprosthesis. *IEEE TRANSACTIONS ON NEURAL SYSTEMS AND REHABILITATION ENGINEERING*, *21*(3), 500–507. https://doi.org/10.1109/TNSRE.2013.2244616

Bjånes, D. A., & Moritz, C. T. (2018). Automated Center-out Rodent Behavioral Trainer (ACRoBaT), an automated device for training rats to perform a modified center out task. *Behavioural Brain Research*, *346*, 115–121. https://doi.org/10.1016/j.bbr.2017.11.031

Brady, A. M., & Floresco, S. B. (2015). Operant Procedures for Assessing Behavioral Flexibility in Rats. *Journal of Visualized Experiments*, (96). https://doi.org/10.3791/52387

Caldwell, D. J., Cronin, J., Wu, J., Kutz, N., Brunton, B., Weaver, K., … Ojemann, J. G. (2017). Spectrotemproal analysis of direct cortical stimulation compared to haptic stimulation in a response time task in humans. Program No. 498.01. 2017 Neuroscience Meeting Planner. Washington, DC: Society for Neuroscience.

Carmena, J. M., Lebedev, M. A., Crist, R. E., O'Doherty, J. E., Santucci, D. M., Dimitrov, D. F., … Nicolelis, M. A. L. (2003). Learning to control a brain-machine interface for reaching and grasping by primates. *PLoS Biology*, *1*(2), 193–208. https://doi.org/10.1371/journal.pbio.0000042

Collinger, J. L., Wodlinger, B., Downey, J. E., Wang, W., Tyler-Kabara, E. C., Weber, D. J., … Schwartz, A. B. (2013). High-performance neuroprosthetic control by an individual with tetraplegia. *The Lancet*, *381*(9866), 557–564. https://doi.org/10.1016/S0140-6736(12)61816-9

Collins, K. L., Guterstam, A., Cronin, J., Olson, J. D., Ehrsson, H. H., & Ojemann, J. G. (2017). Ownership of an artificial limb induced by electrical brain stimulation. *Proceedings of the National Academy of Sciences*, *114*(1), 166–171. https://doi.org/10.1073/pnas.1616305114

Crabbe, J. C. (1999). Genetics of Mouse Behavior: Interactions with Laboratory Environment. *Science*, *284*(5420), 1670–1672. https://doi.org/10.1126/science.284.5420.1670

Cronin, J. A., Wu, J., Collins, K. L., Sarma, D., Rao, R. P. N., Ojemann, J. G., & Olson, J. D. (2016). Task-Specific Somatosensory Feedback via Cortical Stimulation in Humans. *IEEE Transactions on Haptics*, *9*(4), 515–522. https://doi.org/10.1109/TOH.2016.2591952

Dadarlat, M. C., O'Doherty, J. E., & Sabes, P. N. (2015). A learning-based approach to artificial sensory feedback leads to optimal integration. *Nature Neuroscience*, *18*(1), 138–144. https://doi.org/10.1038/nn.3883

Efron, R. (1970). The minimum duration of a perception. *Neuropsychologia*, *8*(1), 57–63. https://doi.org/10.1016/0028-3932(70)90025-4

Endo, T., Maekawa, F., Võikar, V., Haijima, A., Uemura, Y., Zhang, Y., … Kakeyama, M. (2011). Automated test of behavioral flexibility in mice using a behavioral sequencing task in IntelliCage. *Behavioural Brain Research*, *221*(1), 172–181. https://doi.org/10.1016/j.bbr.2011.02.037

Eric Kandel, James Schwartz, T. J.-. (2014). 2000 Principles Of Neural Science-McGraw-Hill Medical (2000). *Igarss 2014*, (1), 1–5. https://doi.org/10.1007/s13398-014-0173-7.2

Fagg, A. H., Hatsopoulos, N. G., de Lafuente, V., Moxon, K. A., Nemati, S., Rebesco, J. M., … Miller, L. E. (2007). Biomimetic Brain Machine Interfaces for the Control of Movement. *Journal of Neuroscience*, *27*(44), 11842–11846. https://doi.org/10.1523/JNEUROSCI.3516-07.2007

Fechner, G. T. (1860). Elements of psychophysics. *Readings in the History of Psychology.*, 206–213. https://doi.org/10.1037/11304-026

Fenrich, K. K., May, Z., Hurd, C., Boychuk, C. E., Kowalczewski, J., Bennett, D. J., … Fouad, K. (2015). Improved single pellet grasping using automated ad libitum full-time training robot. *Behavioural Brain Research*, *281*, 137–148. https://doi.org/10.1016/j.bbr.2014.11.048

Fetz, E. (1969). Operant conditioning of cortical unit activity. *Science*, (February), 28–31. Retrieved from http://www.sciencemag.org/content/163/3870/955.short

Fitzsimmons, N. a, Drake, W., Hanson, T. L., Lebedev, M. a, & Nicolelis, M. a L. (2007). Primate reaching cued by multichannel spatiotemporal cortical microstimulation. *The Journal of Neuroscience : The Official Journal of the Society for Neuroscience*, *27*(21), 5593–5602. https://doi.org/10.1523/JNEUROSCI.5297-06.2007

Flesher, S. N., Collinger, J. L., Foldes, S. T., Weiss, J. M., Downey, J. E., Tyler-Kabara, E. C., … Gaunt, R. A. (2016). Intracortical microstimulation of human somatosensory cortex. *Science Translational Medicine*, *8*(361), 361ra141-361ra141. https://doi.org/10.1126/scitranslmed.aaf8083

Fridman, G., Blair, H., Blaisdell, A., & Judy, J. (2010). Perceived intensity of somatosensory cortical electrical stimulation. *Experimental Brain Research*, 499–515. https://doi.org/10.1007/s00221-010-2254-y

Georgopoulos, a P., Kalaska, J. F., Caminiti, R., & Massey, J. T. (1982). On the relations between the direction of two-dimensional arm movements and cell discharge in primate motor cortex. *J.Neurosci.*, *2(11)*(11), 1527–1537. https://doi.org/citeulike-article-id:444841

Godlove, J. M., Whaite, E. O., & Batista, A. P. (2014). Comparing temporal aspects of visual, tactile, and microstimulation feedback for motor control. *Journal of Neural Engineering*, *11*(4), 046025. https://doi.org/10.1088/1741-2560/11/4/046025

Goodman, S., & Check, E. (2002). The great primate debate. *Nature*, *417*(6890), 684–687. https://doi.org/10.1038/417684a

Goshi, N., Castagnola, E., Vomero, M., Gueli, C., Cea, C., Zucchini, E., … Fadiga, L. (2018). Glassy carbon MEMS for novel origami-styled 3D integrated intracortical and epicortical neural probes. *Journal of Micromechanics and Microengineering*, *28*(6). https://doi.org/10.1088/1361-6439/aab061

Graczyk, E. L., Schiefer, M. A., Saal, H. P., Delhaye, B. P., Bensmaia, S. J., & Tyler, D. J. (2016). The neural basis of perceived intensity in natural and artificial touch. *Science Translational Medicine*, *8*(362). https://doi.org/10.1126/scitranslmed.aaf5187

Hernandez, A., Zainos, A., & Romo, R. (2000). Neuronal correlates of sensory discrimination in the somatosensory cortex. *Proceedings of the National Academy of Sciences*, *97*(11), 6191–6196. https://doi.org/10.1073/pnas.120018597

Hochberg, L. R., Bacher, D., Jarosiewicz, B., Masse, N. Y., Simeral, J. D., Vogel, J., … Donoghue, J. P. (2012). Reach and grasp by people with tetraplegia using a neurally controlled robotic arm. *Nature*, *485*(7398), 372–375. https://doi.org/10.1038/nature11076

Hochberg, L. R., Serruya, M. D., Friehs, G. M., Mukand, J. A., Saleh, M., Caplan, A. H., … Donoghue, J. P. (2006). Neuronal ensemble control of prosthetic devices by a human with tetraplegia. *Nature*, *442*(7099), 164–171. https://doi.org/10.1038/nature04970

Houweling, A. R., & Brecht, M. (2008). Behavioural report of single neuron stimulation in somatosensory cortex. *Nature*, *451*(7174), 65–68. https://doi.org/10.1038/nature06447

Jackson, A., & Fetz, E. E. (2007). Compact movable microwire array for long-term chronic unit recording in cerebral cortex of primates. *Journal of Neurophysiology*, *98*(5), 3109–3118. https://doi.org/10.1152/jn.00569.2007

Johannes, M. S., Bigelow, J. D., Burck, J. M., Harshbarger, S. D., & Kozlowski, M. V. (2011). An Overview of the Developmental Process for the Modular Prosthetic Limb, *30*(3), 207–216.

Johnson, L. A., Wander, J. D., Sarma, D., Su, D. K., Fetz, E. E., & Ojemann, J. G. (2013). Direct electrical stimulation of the somatosensory cortex in humans using electrocorticography electrodes: A qualitative and quantitative report. *Journal of Neural Engineering*, *10*(3). https://doi.org/10.1088/1741-2560/10/3/036021

Kalaska, J. F., Scott, S. H., Cisek, P., & Sergio, L. E. (1997). Cortical control of reaching movements. *Current Opinion in Neurobiology*, *7*, 849–859. https://doi.org/10.1016/S0959-4388(97)80146-8

Kellis, S. S., House, P. A., Thomson, K. E., Brown, R., & Greger, B. (2009). Human neocortical electrical activity recorded on nonpenetrating microwire arrays: applicability for neuroprostheses. *Neurosurgical Focus*, *27*(1), E9. https://doi.org/10.3171/2009.4.FOCUS0974

Kennedy, P. R., & Bakay, R. A. E. (1998). Restoration of neural output from a paralyzed patient by a direct brain connection. *Neuroreport*, *9*(8), 1707–1711. https://doi.org/10.1097/00001756-199806010-00007

Kepecs, A., Uchida, N., Zariwala, H. A., & Mainen, Z. F. (2008). Neural correlates, computation and behavioural impact of decision confidence. *Nature*, *455*(7210), 227–231. https://doi.org/10.1038/nature07200

Kim, S., Callier, T., Bensmaia, S. J., Histed M H, N. A. M. and M. J. H., Schmidt E, B. M. H. F. K. C. O. D. and V. P., Salzman C D, B. K. H. and N. W. T., … Histed M H, B. V. and R. R. C. (2017). A computational model that predicts behavioral sensitivity to intracortical microstimulation. *Journal of Neural Engineering*, *14*(1), 016012. https://doi.org/10.1088/1741-2552/14/1/016012

Kim, S., Callier, T., Tabot, G. A., Gaunt, R. A., Tenore, F. V., & Bensmaia, S. J. (2015). Behavioral assessment of sensitivity to intracortical microstimulation of primate somatosensory cortex. *Proceedings of the National Academy of Sciences*, *112*(49), 15202–15207. https://doi.org/10.1073/pnas.1509265112

Klaes, C., Shi, Y., Kellis, S., Minxha, J., Revechkis, B., & Andersen, R. A. (2014). A cognitive neuroprosthetic that uses cortical stimulation for somatosensory feedback. *Journal of Neural Engineering*, *11*(5), 056024. https://doi.org/10.1088/1741-2560/11/5/056024

Lankau, E. W., Turner, P. V, Mullan, R. J., & Galland, G. G. (2014). Use of Nonhuman Primates in Research in North America. *Journal of the American Association for Laboratory Animal Science : JAALAS*, *53*(3), 278–282. Retrieved from http://www.ncbi.nlm.nih.gov/pmc/articles/PMC4128566/

Lee, B., Kramer, D., Armenta Salas, M., Kellis, S., Brown, D., Dobreva, T., … Andersen, R. A. (2018). Engineering Artificial Somatosensation Through Cortical Stimulation in Humans. *Frontiers in Systems Neuroscience*, *12*, 24. https://doi.org/10.3389/fnsys.2018.00024

London, B. B. M., Jordan, L. R. L., Jackson, C. R., & Miller, L. E. (2008). Electrical stimulation of the proprioceptive cortex (area 3a) used to instruct a behaving monkey. *Neural Systems and …*, *16*(1), 32–36. https://doi.org/10.1109/TNSRE.2007.907544.Electrical

Mackevicius, E. L., Best, M. D., Saal, H. P., & Bensmaia, S. J. (2012). Millisecond precision spike timing shapes tactile perception. *The Journal of Neuroscience : The Official Journal of the Society for Neuroscience*, *32*(44), 15309–15317.

https://doi.org/10.1523/JNEUROSCI.2161-12.2012

Malekmohammadi, M., Herron, J., Velisar, A., Blumenfeld, Z., Trager, M. H., Chizeck, H. J., & Brontë-Stewart, H. (2016). Kinematic Adaptive Deep Brain Stimulation for Resting Tremor in Parkinson's Disease. *Movement Disorders*, *31*(3), 426–428. https://doi.org/10.1002/mds.26482

Marasco, P. D., Kim, K., Colgate, J. E., Peshkin, M. A., & Kuiken, T. A. (2011). Robotic touch shifts perception of embodiment to a prosthesis in targeted reinnervation amputees. *Brain*, *134*(3), 747–758. https://doi.org/10.1093/brain/awq361

Merrill, D. R., Bikson, M., & Jefferys, J. G. R. (2005). Electrical stimulation of excitable tissue: Design of efficacious and safe protocols. *Journal of Neuroscience Methods*, *141*(2), 171–198. https://doi.org/10.1016/j.jneumeth.2004.10.020

Miltenberger, R. G., Perkins, J. A., Weiss, B., Carrington, C., & Williams, A. (2008). Behavioral Modification: Principles and Procedures. *Higher Education*, *4*.

Mohebi, A., & Oweiss, K. G. (2014). A Fully Automated Rodent Conditioning Protocol for Sensorimotor Integration and Cognitive Control Experiments. *Journal of Visualized Experiments*, (86). https://doi.org/10.3791/51128

Moritz, C. T., Perlmutter, S. I., & Fetz, E. E. (2008). Direct control of paralysed muscles by cortical neurons. *Nature*, *456*(7222), 639–642. https://doi.org/10.1038/nature07418

Murphy, R. A., Mondragon, E., & Murphy, V. A. (2008). Rule Learning by Rats. *Science*, *319*(5871), 1849–1851. https://doi.org/10.1126/science.1151564

Murphy, T. H., Boyd, J. D., Bolaños, F., Vanni, M. P., Silasi, G., Haupt, D., & LeDue, J. M. (2016). High-throughput automated home-cage mesoscopic functional imaging of mouse cortex. *Nature Communications*, *7*, 11611. https://doi.org/10.1038/ncomms11611

Musallam, S., Corneil, B. D., Greger, B., Scherberger, H., & Andersen, R. A. (2004). Cognitive control signals for neural prosthetics. *Science*, *305*(5681), 258–262. https://doi.org/10.1126/science.1097938

Nadler, J. J., Moy, S. S., Dold, G., Trang, D., Simmons, N., Perez, A., … Crawley, J. N. (2004). Automated apparatus for quantitation of social approach behaviors in mice. *Genes, Brain and Behavior*, *3*(5), 303–314. https://doi.org/10.1111/j.1601-183X.2004.00071.x

Navarro, X., Krueger, T. B., Lago, N., Micera, S., Stieglitz, T., & Dario, P. (2005). A critical review of interfaces with the peripheral nervous system for the control of neuroprostheses and hybrid bionic systems. *Journal of the Peripheral Nervous System*, *10*(3), 229–258. https://doi.org/10.1111/j.1085-9489.2005.10303.x

Newsome, W. T., Britten, K. H., & Movshon, J. A. (1989). Neuronal correlates of a perceptual decision. *Nature*, *341*(6237), 52–54. https://doi.org/10.1038/341052a0

Nicolelis, M. A. L., & Lebedev, M. A. (2009). Principles of neural ensemble physiology underlying the operation of brain–machine interfaces. *Nature Reviews Neuroscience*, *10*(7), 530–540. https://doi.org/10.1038/nrn2653

O'Doherty, J. E., Lebedev, M. A., Ifft, P. J., Zhuang, K. Z., Shokur, S., Bleuler, H., & Nicolelis, M. A. L. (2011a). Active tactile exploration using a brain-machine-brain interface. *Nature*, *479*(7372), 228–231. https://doi.org/10.1038/nature10489

O'Doherty, J. E., Lebedev, M. A., Ifft, P. J., Zhuang, K. Z., Shokur, S., Bleuler, H., & Nicolelis, M. a L. (2011b). Active tactile exploration using a brain-machine-brain interface. *Nature*, *479*(7372), 228–231. https://doi.org/10.1038/nature10489

Oh, J., & Fitch, W. T. (2017). CATOS (Computer Aided Training/Observing System): Automating animal observation and training. *Behavior Research Methods*, *49*(1), 13–23. https://doi.org/10.3758/s13428-015-0694-9

Ohara, S., Weiss, N., & Lenz, F. a. (2004). Microstimulation in the region of the human thalamic principal somatic sensory nucleus evokes sensations like those of mechanical stimulation and movement. *Journal of Neurophysiology*, *91*(2), 736–745. https://doi.org/10.1152/jn.00648.2003

Ölveczky, B. P. (2011). Motoring ahead with rodents. *Current Opinion in Neurobiology*, *21*(4), 571–578. https://doi.org/10.1016/j.conb.2011.05.002

Penfield, W., & Boldrey, E. (1937). Somatic motor and sensory representation in the cerebral cortex of man as studied by electrical stimulation. *Brain*, *60*(4), 389–443. https://doi.org/10.1093/brain/60.4.389

Platt, M. L., & Glimcher, P. W. (1999). Neural correlates of decision variables in parietal cortex. *Nature*, *400*(6741), 233–238. https://doi.org/10.1038/22268

Poddar, R., Kawai, R., & Ölveczky, B. P. (2013). A fully automated high-throughput training system for rodents. *PLoS ONE*, *8*(12). https://doi.org/10.1371/journal.pone.0083171

Rajan, A. T., Boback, J. L., Dammann, J. F., Tenore, F. V., Wester, B. A., Otto, K. J., … Bensmaia, S. J. (2015). The effects of chronic intracortical microstimulation on neural tissue and fine motor behavior. *Journal of Neural Engineering*, *12*(6), 66018. https://doi.org/10.1088/1741-2560/12/6/066018

Raposo, D., Sheppard, J. P., Schrater, P. R., & Churchland, A. K. (2012). Multisensory Decision-Making in Rats and Humans. *Journal of Neuroscience*, *32*(11), 3726–3735. https://doi.org/10.1523/JNEUROSCI.4998-11.2012

Resnik, L., Klinger, S. L., & Etter, K. (2014). The DEKA Arm: Its features, functionality, and evolution during the veterans affairs study to optimize the DEKA Arm. *Prosthetics and Orthotics International*, *38*(6), 492–504. https://doi.org/10.1177/0309364613506913

Riso, R. R. (1999). Strategies for providing upper extremity amputees with tactile and hand

position feedback--moving closer to the bionic arm. *Technology and Health Care : Official Journal of the European Society for Engineering and Medicine*, *7*(6), 401–409. https://doi.org/10.1080/09640560701402075

Romo, R., Hernández, A., Zainos, A., Brody, C. D., & Lemus, L. (2000). Sensing without touching: Psychophysical performance based on cortical microstimulation. *Neuron*, *26*(1), 273–278. https://doi.org/10.1016/S0896-6273(00)81156-3

Romo, R., Hernández, A., Zainos, A., & Salinas, E. (1998). Somatosensory discrimination based on cortical microstimulation. *Nature*, *392*(March), 387–390. Retrieved from http://www.nature.com/nature/journal/v392/n6674/abs/392387a0.html

Santhanam, G., Ryu, S. I., Yu, B. M., Afshar, A., & Shenoy, K. V. (2006). A high-performance brain–computer interface. *Nature*, *442*(7099), 195–198. https://doi.org/10.1038/nature04968

Schaefer, A. T., & Claridge-Chang, A. (2012). The surveillance state of behavioral automation. *Current Opinion in Neurobiology*, *22*(1), 170–176. https://doi.org/10.1016/j.conb.2011.11.004

Schafer E. A. (1888). Experiments on the electrical excitation of the cerebral cortex in the monkey. *Brain*, *11*, 1–6.

Schalk, G., McFarland, D. J., Hinterberger, T., Birbaumer, N., & Wolpaw, J. R. (2004). BCI2000: A general-purpose brain-computer interface (BCI) system. *IEEE Transactions on Biomedical Engineering*, *51*(6), 1034–1043. https://doi.org/10.1109/TBME.2004.827072

Serruya, M. D., Hatsopoulos, N. G., Paninski, L., Fellows, M. R., & Donoghue, J. P. (2002). Instant neural control of a movement signal. *Nature*, *416*(6877), 141–142. https://doi.org/10.1038/416141a

Shadlen, M. N., & Newsome, W. T. (2001). Neural Basis of a Perceptual Decision in the Parietal Cortex (Area LIP) of the Rhesus Monkey. *Journal of Neurophysiology*, *86*(4), 1916–1936. https://doi.org/10.1152/jn.2001.86.4.1916

Shannon, R. V. (1992). A Model of Safe Levels for Electrical Stimulation. *IEEE Transactions on Biomedical Engineering*, *39*(4), 424–426. https://doi.org/10.1109/10.126616

Slutzky, M., & Jordan, L. (2010). A new rodent behavioral paradigm for studying forelimb movement. *Journal of Neuroscience …*, *192*(2), 228–232. https://doi.org/10.1016/j.jneumeth.2010.07.040.A

Smith, C. U. M. (2009). *Biology of Sensory Systems*. https://doi.org/10.1002/9780470694374

Sunshine, M. D., Cho, F. S., Lockwood, D. R., Fechko, A. S., Kasten, M. R., & Moritz, C. T. (2013). Cervical intraspinal microstimulation evokes robust forelimb movements before and after injury. *Journal of Neural Engineering*, *10*(3), 036001. https://doi.org/10.1088/1741-2560/10/3/036001

Tabot, G. A., Dammann, J. F., Berg, J. A., Tenore, F. V., Boback, J. L., Vogelstein, R. J., & Bensmaia, S. J. (2013). Restoring the sense of touch with a prosthetic hand through a brain interface. *Proceedings of the National Academy of Sciences of the United States of America*, *110*(45), 18279–18284. https://doi.org/10.1073/pnas.1221113110

Tan, D. W., Schiefer, M. A., Keith, M. W., Anderson, J. R., Tyler, J., & Tyler, D. J. (2014). A neural interface provides long-term stable natural touch perception. *Science Translational Medicine*, *6*(257). https://doi.org/10.1126/scitranslmed.3008669

Tanji, J. (2001). Sequential Organization of Multiple Movements: Involvement of Cortical Motor Areas. *Annual Review of Neuroscience*, *24*(1), 631–651. https://doi.org/10.1146/annurev.neuro.24.1.631

Taylor, D. M. (2002). Direct Cortical Control of 3D Neuroprosthetic Devices. *Science*, *296*(5574), 1829–1832. https://doi.org/10.1126/science.1070291

Tehovnik, E. (1996). Electrical stimulation of neural tissue to evoke behavioral responses. *Journal of Neuroscience Methods*, *65*(1), 1–17. Retrieved from http://www.ncbi.nlm.nih.gov/pubmed/8815302

Thomson, E. E., Carra, R., & Nicolelis, M. a L. (2013). Perceiving invisible light through a somatosensory cortical prosthesis. *Nature Communications*, *4*, 1482. https://doi.org/10.1038/ncomms2497

Torres-Espín, A., Forero, J., Schmidt, E. K. A., Fouad, K., & Fenrich, K. K. (2018). A motorized pellet dispenser to deliver high intensity training of the single pellet reaching and grasping task in rats. *Behavioural Brain Research*, *336*, 67–76. https://doi.org/10.1016/j.bbr.2017.08.033

Uchida, N., & Mainen, Z. F. (2003). Speed and accuracy of olfactory discrimination in the rat. *Nature Neuroscience*, *6*(11), 1224–1229. https://doi.org/10.1038/nn1142

Velliste, M., Perel, S., Spalding, M. C., Whitford, A. S., & Schwartz, A. B. (2008). Cortical control of a prosthetic arm for self-feeding. *Nature*, *453*(7198), 1098–1101. https://doi.org/10.1038/nature06996

Venkatraman, S., & Carmena, J. (2009). Behavioral modulation of stimulus-evoked oscillations in barrel cortex of alert rats. *Frontiers in Integrative …*, *3*(June), 1–10. https://doi.org/10.3389/neuro.07

Viana, D. S., Gordo, I., Sucena, É., & Moita, M. A. P. (2010). Cognitive and Motivational Requirements for the Emergence of Cooperation in a Rat Social Game. *PLoS ONE*, *5*(1), e8483. https://doi.org/10.1371/journal.pone.0008483

Viventi, J., Kim, D. H., Vigeland, L., Frechette, E. S., Blanco, J. A., Kim, Y. S., … Litt, B. (2011). Flexible, foldable, actively multiplexed, high-density electrode array for mapping brain activity in vivo. *Nature Neuroscience*, *14*(12), 1599–1605. https://doi.org/10.1038/nn.2973

Wang, W., Collinger, J. L., Degenhart, A. D., Tyler-Kabara, E. C., Schwartz, A. B., Moran, D. W., … Boninger, M. L. (2013). An Electrocorticographic Brain Interface in an Individual with Tetraplegia. *PLoS ONE*, *8*(2). https://doi.org/10.1371/journal.pone.0055344

Watson, G. P. and C., Paxinos, G., & Charles, W. (2005). *The rat brain in stereotaxic coordinates*.

Weber, A. I., Saal, H. P., Lieber, J. D., Cheng, J.-W., Manfredi, L. R., Dammann, J. F., & Bensmaia, S. J. (2013). Spatial and temporal codes mediate the tactile perception of natural textures. *Proceedings of the National Academy of Sciences of the United States of America*, *110*(42), 17107–17112. https://doi.org/10.1073/pnas.1305509110

Weber, D. J., Stein, R. B., Everaert, D. G., & Prochazka, A. (2007). Limb-state feedback from ensembles of simultaneously recorded dorsal root ganglion neurons. *Journal of Neural Engineering*, *4*(3). https://doi.org/10.1088/1741-2560/4/3/S04

Wessberg, J., Stambaugh, C. R., Kralik, J. D., Beck, P. D., M.Laubach, Chapin, J. K., … Biggs, S. J. (2000). Real-time prediction of hand tranjectory by ensembles of cortical neurons in primate. *Nature*, *408*(1), 361–365.

Whishaw, I. Q., Gorny, B., Foroud, A., & Kleim, J. A. (2003). Long-Evans and Sprague-Dawley rats have similar skilled reaching success and limb representations in motor cortex but different movements: Some cautionary insights into the selection of rat strains for neurobiological motor research. *Behavioural Brain Research*, *145*(1–2), 221–232. https://doi.org/10.1016/S0166-4328(03)00143-8

Widge, A. S., Dougherty, D. D., & Moritz, C. T. (2014). Affective brain-computer interfaces as enabling technology for responsive psychiatric stimulation. *Brain-Computer Interfaces*, *1*(2), 126–136. https://doi.org/10.1080/2326263X.2014.912885

Wong, C. C., Ramanathan, D. S., Gulati, T., Won, S. J., & Ganguly, K. (2015). An automated behavioral box to assess forelimb function in rats. *Journal of Neuroscience Methods*, *246*, 30–37. https://doi.org/10.1016/j.jneumeth.2015.03.008

Zeeb, F. D., Robbins, T. W., & Winstanley, C. A. (2009). Serotonergic and Dopaminergic Modulation of Gambling Behavior as Assessed Using a Novel Rat Gambling Task. *Neuropsychopharmacology*, *34*(10), 2329–2343. https://doi.org/10.1038/npp.2009.62

Zemmar, A., Kast, B., Lussi, K., Luft, A. R., & Schwab, M. E. (2015). Acquisition of a High-precision Skilled Forelimb Reaching Task in Rats. *Journal of Visualized Experiments*, (100). https://doi.org/10.3791/53010

Zheng, W., & Ycu, E. A. (2012). A Fully Automated and Highly Versatile System for Testing Multi-cognitive Functions and Recording Neuronal Activities in Rodents. *Journal of Visualized Experiments*, (63). https://doi.org/10.3791/3685

Zoccolan, D., Oertelt, N., DiCarlo, J. J., & Cox, D. D. (2009). A rodent model for the study of invariant visual object recognition. *Proceedings of the National Academy of Sciences*,

106(21), 8748–8753. https://doi.org/10.1073/pnas.0811583106

VITA

David Bjånes is completing his Ph.D. studies in Electrical Engineering at the University of Washington. His research focuses on brain machine interfaces and restoring loss of somatosensation through direct electrical stimulation of the sensorimotor cortex. By establishing a low-latency, high-resolution artificial sensory feedback channel, brain computer interfaces users could have more robust control over prosthetics limbs, peripheral nerve interfaces and restore a primary method of interacting with their world.

David previously received a master's degree in Electrical and Computer Engineering from the University of Pittsburgh, studying machine learning techniques for analyzing neural signals. His bachelor's degree in Electrical and Computer Engineering is from Cornell University.